includes the bending mode frequency.

$$\cos\Theta = \frac{m_2 m_2'}{2}\,\frac{\dfrac{d_2}{d_1}\left(\dfrac{1}{\mu_1'} - \dfrac{R_\nu R_m}{\mu_1}\right) + \dfrac{d_1}{d_2}\left(\dfrac{1}{\mu_2'} - \dfrac{R_\nu R_m}{\mu_2}\right)}{m_2 - m_2' R_\nu R_m} \quad \cdots \quad (4)$$

$$R_\nu = \left[\frac{\nu_1'\nu_2'\nu_3'}{\nu_1\nu_2\nu_3}\right]^2 \qquad R_m = (M'/M)^2$$

$$\frac{1}{\mu_1} = \frac{1}{m_1} + \frac{1}{m_2} \qquad \frac{1}{\mu_2} = \frac{1}{m_2} + \frac{1}{m_3}$$

Unfortunately, eq 4 is essentially useless for calculating Θ because R_ν depends very weakly on Θ. Thus, ^{13}C substitution gives calculated values of R_ν = 0.879, 0.881, and 0.889 for Θ = 180, 135, and 90°, while ^{18}O substitution gives R_ν = 0.888, 0.887, and 0.876. The entire range of variation is only 1.1%. On the other hand, a measurement error of only 2 cm^{-1} in either ν_{FeC} or in δ_{FeCO}, well within the usual uncertainty since their RR bands are frequently weak and overlapped with porphyrin bands, produces a ~0.8% error in R. Moreover, the equation remains only approximate since all interaction force constants are neglected; it is known from the $Fe(CO)_5$ vibrational analysis that the FeC,CO stretch–stretch interaction constant is not negligible.[33] When the available ^{13}C isotopic data are examined (Table II), the experimental values of R_ν mostly fall in the range of 0.891–0.902, significantly above the highest calculated value, R_ν = 0.889 for Θ = 90°. Probably this systematic upward shift is associated with the FeC,CO interaction constant. The required correction for this effect adds to the utility of the isotopic shifts in determining the FeCO angle directly.

We conclude that it is not possible to calculate the FeCO angle directly from the vibrational frequencies and isotope shifts. These have to be modeled with a specific force field.

The Reaction of *n*-Butyllithium with Diphenylacetylene: Structure Elucidation of the Mono- and Dilithio Product by One- and Two-Dimensional NMR Spectroscopy, X-ray Analysis, and MNDO Calculations. Agostic Activation by Lithium†

Walter Bauer,‡ Martin Feigel,‡ Gerhard Müller,§ and Paul von Ragué Schleyer*,‡

Contribution from the Institute of Organic Chemistry of the Friedrich-Alexander-Universität Erlangen-Nürnberg, Henkestrasse 42, D-8520 Erlangen, Federal Republic of Germany, and the Institute of Inorganic Chemistry of the Technische Universität München, Lichtenbergstr. 4, D-8046 Garching, Federal Republic of Germany. *Received November 13, 1987*

Abstract: One equivalent of *n*-butyllithium (*n*BuLi) adds to diphenylacetylene (tolane) in tetrahydrofuran (THF) to give the trans product **2** exclusively; this monolithio compound is monomeric in THF. When carried out in hexane/TMEDA solution (TMEDA = *N,N,N',N'*-tetramethylethylenediamine), this reaction is accompanied by the formation of the dilithio product **3**. Both **2** and **3** are characterized by two-dimensional NMR spectroscopy (COSY, C–H shift correlation, COLOC). The known site of the second metalation (H8 in **2**) is "predicted" both by ^1H–^6Li–2D heteronuclear Overhauser spectroscopy (HOESY) and by MNDO calculations, both of which indicate a short Li···H8 distance in **2** ("agostic" interaction). The dimetalation product **3** can be obtained directly in hexane/TMEDA with 2 equiv of *n*BuLi. In the crystalline state, **3** is a doubly lithium bridged monomer chelated with one TMEDA ligand per lithium atom (X-ray). The doubly lithium bridged structure is retained in benzene-d_6 solution. In THF-d_8, however, a temperature and concentration dependent monomer–dimer equilibrium is observed ($\Delta H°$ = 9.4 kcal/mol, $\Delta S°$ = 22.2 eu). In the dimer **24**, comprised of a central C_4Li_4 cubic moiety, two pairs of nonisochronous lithium atoms give rise to two signals in the ^6Li NMR spectrum; these are assigned by ^1H–^6Li–2D HOESY. Line shape analysis of the temperature dependent ^6Li spectra gives the activation parameters, $\Delta H^‡$ = 9.4 kcal/mol and $\Delta S^‡$ = −23.5 eu, for the dimer–monomer reaction, whereas the exchange of the chemically nonequivalent lithium sites in the dimer proceeds with $\Delta H^‡$ = 16.1 kcal/mol and $\Delta S^‡$ = 1.2 eu. The lithium exchange within the dimer and in the monomer–dimer equilibrium is proven by 2D–^6Li exchange spectroscopy (NOESY). Small scalar couplings between the chemically nonequivalent ^6Li atoms in the dimer **24** are detected by ^6Li–^6Li COSY.

Organolithium compounds are known to add stereo- and regiospecifically to carbon–carbon double and triple bonds.[1] Such reactions have long been used to initiate polymerization[1] and for the synthesis of many otherwise unavailable functionalized alkanes and alkenes.[1-3] The reaction between *n*-butyllithium (*n*BuLi) and diphenylacetylene (**1**) (tolane), studied extensively 2 decades ago by Mulvaney et al.[4-7] was found not only to give **2** but also to proceed beyond the addition stage. Deuteriation and carbonation experiments gave evidence for the formation of a dilithio compound **3** (Scheme I) as well.

The reaction in hexane was accelerated appreciably by the presence of *N,N,N',N'*-tetramethylethylenediamine, TMEDA.[7] An elegant chemical study[6] demonstrated that the mechanism

† Dedicated to Professor Dr. Valentin Freise, University of Regensburg, Federal Republic of Germany, on the occasion of his 70th birthday.

‡ University of Erlangen-Nürnberg.

§ Technical University of Munich.

(1) Wakefield, B. J. *The Chemistry of Organolithium Compounds*; Pergamon: 1974; p 89f.
(2) Wakefield, B. J. In Wilkinson, G., Stone, F. G. A., Abel, E. W., Eds.; *Comprehensive Organometallic Chemistry*; Pergamon: Oxford, 1982; Vol 7, p 1f.
(3) Normant, J. F.; Alexakis, A. *Synthesis* **1981**, 841.
(4) Mulvaney, J. E.; Garlund, Z. G.; Garlund, S. L. *J. Am. Chem. Soc.* **1963**, *85*, 3897.
(5) Mulvaney, J. E.; Garlund, Z. G.; Garlund, S. L.; Newton, D. J. *J. Am. Chem. Soc.* **1966**, *88*, 476.
(6) Mulvaney, J. E.; Carr, L. J. *J. Org. Chem.* **1968**, *33*, 3286.
(7) Mulvaney, J. E.; Newton, D. J. *J. Org. Chem.* **1969**, *34*, 1936.

0002-7863/88/1510-6033$01.50/0

Scheme I

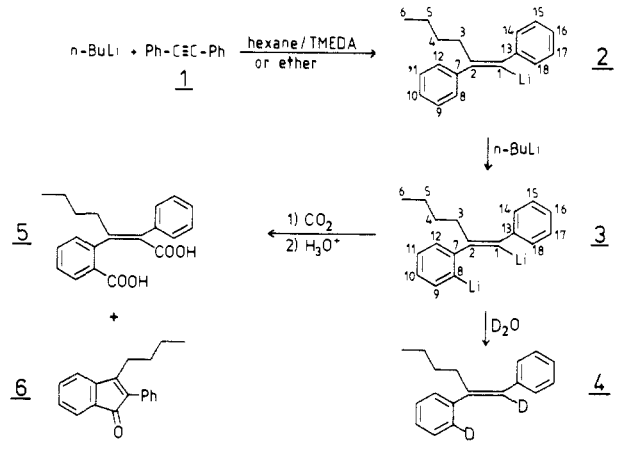

involves the stepwise addition–metalation sequence (shown in Scheme I). The initial cis addition product **7** was postulated to

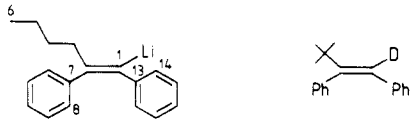

7

8

isomerize[4] to the thermodynamically more stable trans isomer **3**. This assumption is supported by the finding that *tert*-butyllithium reacts with **1** to give the cis isomer **8** as the major product. Ab initio calculations on the addition reaction of lithium hydride to acetlyene predict a syn mechanism consistent with Mulvaney's experimental findings.[8]

The configurational stability of substituted vinyllithium compounds depends to a considerable extent on the substituents and on the solvent.[3] Whereas α-alkyl substituted *cis*-vinyllithium compounds do not undergo cis–trans isomerization,[9,10] vinyllithium derivatives substituted with aryl substituents in the α-position are much more labile toward stereomutation.[9] Among such aryl-substituted compounds, the rate of isomerization in different solvents decreases in the order TMEDA > DME (dimethoxyethane) > THF > diethyl ether > hydrocarbons.[11,12] Knorr and Lattke[13] found exchange of the methyl signals in the ^{1}H NMR spectrum of **9** (equivalent to "cis–trans" isomerization) in THF to be rapid even at −25 °C. A linear phenyl-stabilized vinyl anion transition state with dissociated lithium was postulated for this process.

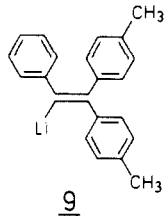

9

Our initial interest in the reaction of Scheme I focused on the trans addition product **2**. According to earlier theoretical predictions,[14] the ortho hydrogen atoms H8,12 of the aromatic ring att C2 in **2** were expeected to be activated specifically toward

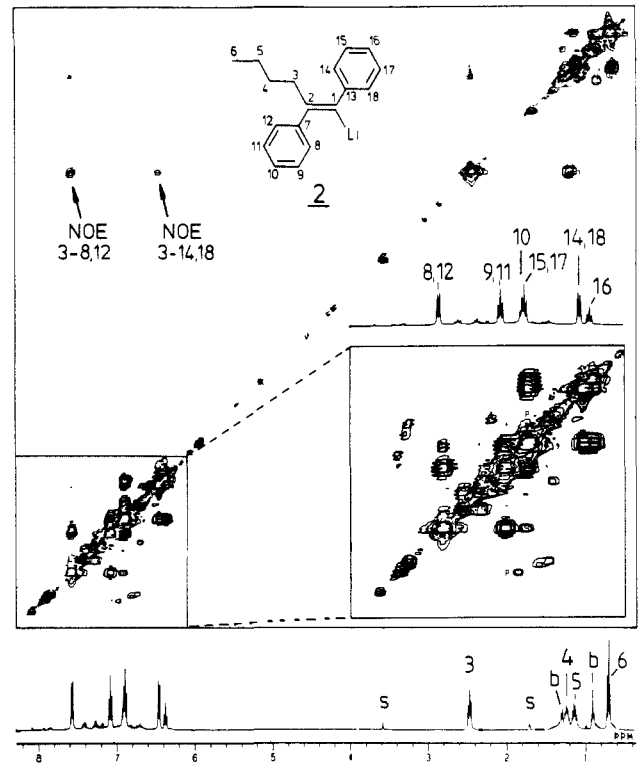

Figure 1. (*E*)-1-Lithio-1,2-diphenylhex-1-ene (**2**), the addition product of *n*-BuLi and tolane, in situ preparation, ^{1}H–^{1}H COSY (below diagonal) and NOESY (above diagonal), THF-d_8, −5 °C, 0.7 M, combined COSY–NOESY pulse sequence ("COCONOESY"[15]) mixing time 700 ms with statistical ±5% variation; b = butane; s = solvent; insert: COSY plot of section indicated.

further metalation, e.g., more so than the seemingly analogous positions H14,18 of the phenyl group at C-1. This interpretation has now been verified experimentally both by NMR spectroscopy and by X-ray analysis. Augmented by MNDO calculations, these methods not only provided answers to the main questions but also revealed many interesting additional structural details as well.

Results and Discussion

Monolithioproduct 2. ^{1}H NMR. Addition of 1 equiv of *n*BuLi to a tolane–THF solution at 0 °C results in appearance of a dark green color. When the reactants are combined in an NMR tube at −40 °C and slowly allowed to warm while monitoring the reaction course by means of ^{1}H NMR, the tolane and *n*-BuLi signals disappear slowly at $T > -20$ °C, and new peaks appear simultaneously. The reaction is complete after ca. 4 h at −5 °C. The ^{1}H NMR spectrum (Figure 1) shows only one *addition* product to be present; a single set of signals, consistent with structure **2** predominates. However, minor side reactions, probably from ring metalation products of tolane are indicated in Figure 1 by additional small peaks in the aromatic region and those due to butane. A vinyllithium–allyllithium isomerization in THF at 0 °C has been found[16] (Scheme II) for α-phenyl-β,β-dimethylvinyllithium (**10**) (a system comparable to **2** but with aliphatic substituents in the β-position); H1 in the rearranged species **11** resonates at $\delta = 3.8$ ppm.[16] The lack of a signal in this region in Figure 1 shows such an isomerization has not occurred with the addition product **2** under these conditions.

The signal pattern in the aromatic region of Figure 1 shows only three characteristic signals for each phenyl ring, i.e., pairwise isochronicity for corresponding ortho and meta signals; hence, the phenyl substituents are rotating rapidly. On cooling to −90 °C, the ^{1}H NMR spectrum of **2** remains unchanged. This indicates

(8) Houk, K. N.; Rondan, N. G.; Schleyer, P. v. R.; Kaufmann, E.; Clark, T. *J. Am. Chem. Soc.* **1985**, *107*, 2821.
(9) Wardell, J. L. In Wilkinson, G., Stone, F. G. A., Abel, E. W., Eds.; *Comprehensive Organometallic Chemistry*; Pergamon: Oxford, 1982; Vol. 1, p 94f.
(10) Seyferth, D.; Vaughan, L. G. *J. Am. Chem. Soc.* **1964**, *86*, 883.
(11) Panek, E. J.; Neff, B. L.; Chu, H.; Panek, M. G. *J. Am. Chem. Soc.* **1975**, *97*, 3996.
(12) Curtin, D. Y.; Koehl, W. J., Jr. *J. Am. Chem. Soc.* **1962**, *84*, 1967.
(13) Knorr, R.; Lattke, E. *Tetrahedron Lett.* **1977**, 3969.
(14) Neugebauer, W.; Kos, A. J.; Schleyer, P. v. R. *J. Organomet. Chem.* **1982**, *228*, 107. Neugebauer, W.; Clark, T.; Schleyer, P. v. R. *Chem. Ber.* **1983**, *116*, 3283.
(15) Haasnoot, C. A. G.; Van de Ven, F. J. M.; Hilbers, C. W. *J. Magn. Reson.* **1984**, *56*, 343. Gurevich, A. Z.; Barsukov, I. L.; Arseniev, A. S.; Bystrov, V. F. *J. Magn. Reson.* **1984**, *56*, 471. NM Group, *JEOL News* **1985**, *21A*, 8.
(16) Knorr, R.; Lattke, E. *Tetrahedron Lett.* **1977**, 4655, 4659.

Table I. ^{1}H NMR Chemical Shifts (δ, ppm), Multiplicities,[25] and Coupling Constants (Hz) for **2**[a]

H				
3	2.47	t	7.6 Hz	
4	1.24	tt	7.6 Hz	7.4 Hz
5	1.14	qt	7.4 Hz	7.4 Hz
6	0.71	t	7.4 Hz	
8/12	7.57	d	7.2 Hz	
9/11	7.08	dd	7.2 Hz	7.2 Hz
10	6.91	t	7.2 Hz	
14/18	6.46	d	7.2 Hz	
15/17	6.89	dd	7.2 Hz	7.2 Hz
16	6.38	t	7.2 Hz	

[a] THF-d_8, −5 °C, in situ preparation, 0.7 M; for numbering see formula in text and in Figure 1.

either a mixture of rapidly equilibrating aggregates even at this low temperature or, more likely, only one species to be present. This species is the monomer **2** (as will be discussed below) which has low rotation barriers for both phenyl rings.

The ^{1}H connectivities for the *n*-butyl group signals and for the signals of the separate aromatic rings can be extracted from the COSY[17,18] plot in Figure 1. However, the differentiation between the two aromatic rings and a proof for the trans geometry of the addition product **2** does not follow directly from the COSY spectrum. However, the corresponding NOESY[19,20] plot reveals spatial proximities between protons; note the cross peaks (arrows in Figure 1) between the allylic protons H3 and the ortho protons H8,12 (intense) and H14,18 (weaker). These observations are incompatible with a cis product **7**, since the ortho hydrogen atoms of the aromatic ring trans to the alkyl group (H14/18) would be too remote to interact with H3. Hence, we conclude that the initial cis addition product **7** of *n*BuLi and tolane isomerizes rapidly under these conditions (THF-d_8, −5 °C) to the thermodynamically more stable *trans*-**2**, possibly (following Knorr's suggestion[13]) via a nearly linear ion pair transition state **12**.

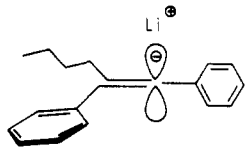

12

Molecular models of **2** indicate the aromatic ortho hydrogen atom H8 to be in much closer proximity to the lithium substituent than is the corresponding ortho hydrogen (H18) of the α-phenyl ring. As has been demonstrated, e.g., for 2-lithio-*N*-phenylpyrrole[21] (**13**) and for 1-lithionaphthalene[22] (**14**), spatial proximity

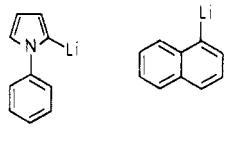

13

14

of lithium and hydrogen ("agostic interactions")[23] result in pronounced *downfield* shifts in the ^{1}H NMR spectrum. This behavior might be explained by the electric field produced by the Li cation and the relative orientations of the CH bond with regard to the lithium cation.[24] Hence, the prominent doublet at 7.57 ppm in

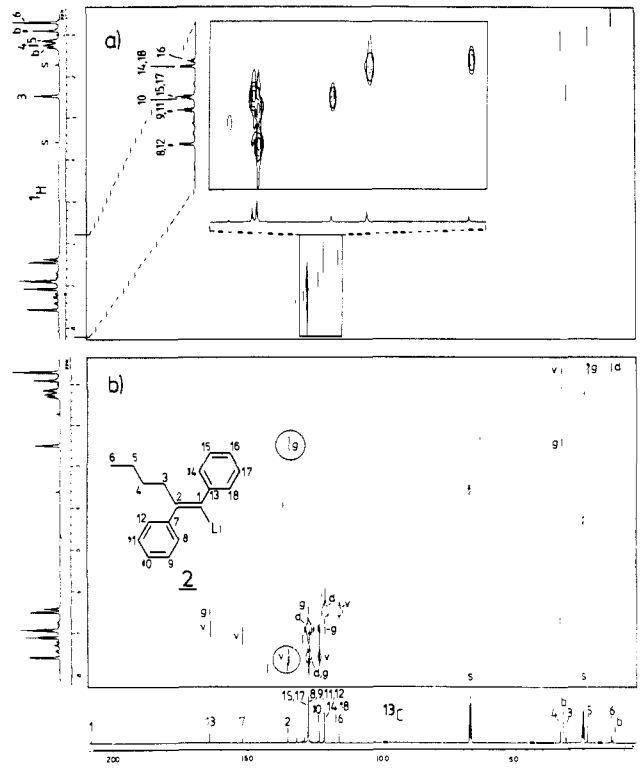

Figure 2. C–H shift correlated spectrum of **2**, THF-d_8, −91 °C, 0.7 M, in situ preparation; b = butane, s = solvent: (a) delays in the pulse sequence optimized for direct couplings ($^1J_{13C,1H}$) and (b) delays in the pulse sequence optimized for long-range couplings. Indications at cross peaks: d (direct coupling, $^1J_{13C,1H}$); g (geminal coupling, $^2J_{13C,1H}$); v (vicinal coupling, $^3J_{13C,1H}$).

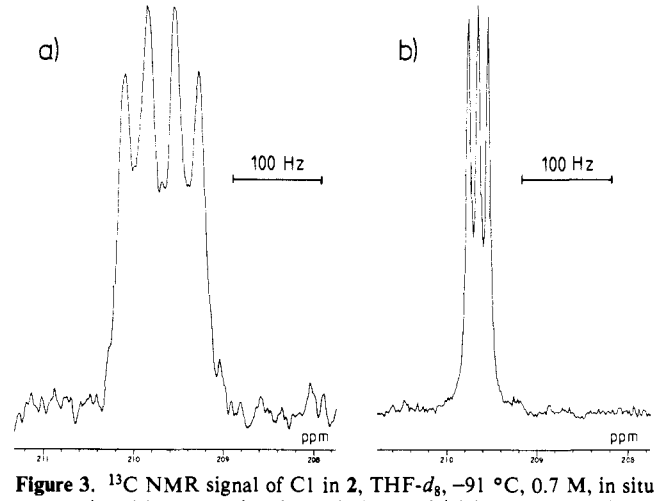

Figure 3. ^{13}C NMR signal of C1 in **2**, THF-d_8, −91 °C, 0.7 M, in situ preparation; (a) natural abundance lithium and (b) isotopically enriched with 96% ^{6}Li.

Figure 1 is due to the ortho hydrogen atoms H8,12 in **2**; this leads (via COSY) to the assignments shown in Figure 1. These assignments are corroborated by the results from ^{1}H–^{6}Li heteronuclear Overhauser spectroscopy (HOESY) (see below). In contrast, the ortho hydrogen atoms H14,18 of the phenyl ring at C1 in **2** resonate at higher field at the "usual" chemical shift value (δ = 6.46 ppm). Table I summarizes the ^{1}H chemical shifts and coupling constants of **2**.

^{13}C NMR. The ^{13}C NMR spectra show the behavior of **2** with regard to aggregation. At −90 °C only one set of signals is found (Figure 2). The resonance of the metalated carbon atom is split into a 1:1:1:1 quartet, J = 28.0 Hz, when *n*BuLi with Li in natural abundance is used for the preparation of **2** (Figure 3a). This is

(17) Aue, W. P.; Bartholdi, E.; Ernst, R. R. *J. Chem. Phys.* **1976**, *64*, 2229.
(18) Morris, G. A. *Magn. Res. Chem.* **1986**, *24*, 371.
(19) Jeener, J.; Meier, B. H.; Bachmann, P.; Ernst, R. R. *J. Chem. Phys.* **1979**, *71*, 4546. Macura, S.; Ernst, R. R. *Mol. Phys.* **1980**, *41*, 95.
(20) Benn, R.; Günther, H. *Angew. Chem., Int. Ed. Engl.* **1983**, *22*, 390.
(21) Bauer, W.; Müller, G.; Pi, R.; Schleyer, P. v. R. *Angew. Chem., Int. Ed. Engl.* **1986**, *25*, 1103.
(22) Bauer, W.; Clark, T.; Schleyer, P. v. R. *J. Am. Chem. Soc.* **1987**, *109*, 970.
(23) Erker, G.; Frömberg, W.; Angermund, K.; Schlund, R.; Krüger, C. *Chem. Commun.* **1986**, 372. Brookhart, M.; Green, M. L. H. *J. Organomet. Chem.* **1983**, *250*, 395. Koga, N.; Obara, S.; Morokuma, K. *J. Am. Chem. Soc.* **1984**, *106*, 4625.
(24) Musher, J. I. *J. Chem. Phys.* **1962**, *37*, 34.

due to coupling of ^{13}C with only *one* ^{7}Li atom (spin $I = 3/2$, natural isotope abundance 92.6%). When *n*BuLi isotopically enriched with ^{6}Li (spin $I = 1$, natural isotope abundance 7.4%)[26,28] is used for the preparation of **2**, the same signal is split into a 1:1:1 triplet, $J = 10.6$ Hz (Figure 3b).[27] This indicates **2** to be monomeric under these conditions.[26,28,29]

The ^{13}C chemical shift of C1 in **2** is unusually high ($\delta = 209.7$ ppm) compared to vinyllithium ($\delta = 186.3$ ppm[29]) and to the vinyllithium derivative **15** ($\delta = 173.5$ ppm[26]). This is due in part

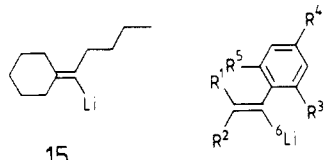

15 16

to the presence of two phenyl groups (cf. ethylene, $\delta = 123.5$ ppm; *trans*-stilbene, $\delta = 137.6$ ppm[30]). In addition, ^{13}C NMR shifts of the metalated carbon atom in lithioorganic compounds have been found to increase with decrease in aggregation[31] (e.g., phenyllithium monomer, $\delta = 196.7$;[31] dimer, $\delta = 188.5$;[26,31] tetramer, $\delta = 176.2$ ppm[32]). The reason for the generally larger ^{13}C chemical shifts of the lithiated carbon atoms in vinyl- and aryllithium compounds as compared to the corresponding hydrocarbons has been attributed by Seebach to increased σ-electron density.[26] According to Fraenkel et al.[33] charge polarization, variations in the π-bond order, and the mean excitation energy for magnetic mixing of π^*-excited states and the ground state are the factors which govern ^{13}C chemical shifts. The latter effect (which opposes the first) was claimed to be responsible for the large downfield shift of C1 in phenyllithium as compared to benzene; the lithiated carbon atom in **2** should behave similarly.

The magnitude of the coupling constant $^{1}J_{13C,6,7Li}$ for C1 in **2** is surprisingly low. From a summary of literature data, the values for $^{1}J_{13C,6,7Li}$ have been found to show the dependence on the degree of aggregation[31] given by eq 1 and 2, where n represents the

$$J_{13C,7Li} = 1/n(45 \pm 5)\ \text{Hz} \quad (1)$$

$$J_{13C,6Li} = 1/n(17 \pm 2)\ \text{Hz} \quad (2)$$

number of lithium atoms bound directly to carbon (in the NMR time scale). While these relationships are obeyed closely by aggregates, deviations are found for monomers. Of the available data, monomeric *tert*-butyllithium and *sec*-butyllithium[31] in THF show $J_{13C,7Li} = 31.5$ and 36.6 Hz, respectively. Moreover, $J_{13C,7Li} = 28.0$ Hz for monomeric **2** is even lower and is in fact closer to the values generally found for dimers. A number of monomeric vinyllithium compounds studied by Knorr and co-workers[34] are similar in this respect. Available $^{13}C,^{6}Li$ coupling constants for monomeric vinyllithium derivatives are summarized in Table III.

Table II. ^{13}C NMR Chemical Shifts of **2**[d]

C	−5 °C	−91 °C
1	208.2[a]	209.7[b]
2	135.0	133.5
3	31.5	31.3
4	33.6	33.4
5	23.6	23.8
6	14.8	15.1
7	152.0	150.8
8, 12	127.3	127.3[c]
9,11	127.3	126.8[c]
10	123.3	123.4
13	164.1	164.0
14, 18	121.4	120.8
15, 17	127.6	127.5[c]
16	116.0	115.6

[a] Sharp singlet. [b] $J_{13C,7Li} = 28.3$ Hz. [c] Assignments may be interchanged; for numbering see formula in text and in Figure 2. [d] THF-d_8, in situ preparation, 0.7 M, natural abundance lithium.

At present we can provide only tentative explanations for these observations: Benzyllithium derivatives at one extreme among organolithium monomers do not show any $^{13}C,^{6}Li$ coupling at temperatures down to −140 °C.[26,35] These are believed to be π-bound "contact ion pairs,"[26,36] wherein any covalent bonding utilizes predominately p rather than s orbitals of lithium. ^{1}H–^{6}Li HOESY measurements hint that the lithium cation in benzyllithium compounds (e.g., fluorenyllithium and 1-phenyl-1-lithioethane) in THF may not be attached closely to the hydrocarbon anion.[35] Depending on the structure, it is possible that there is a variable change from tightly to loosely bound lithium in monomers, but this is not the case for organolithium aggregates.

The C2–C18 ^{13}C NMR resonances for **2**, obtained from C–H shift correlation spectroscopy[18,37] (Figure 2), are summarized in Table II. The signals of the carbon atoms bearing protons show cross peaks (Figure 2a); these allow unambiguous assignment in conjugation with the previously analyzed ^{1}H NMR spectrum. The accidental coincidence of the ortho and the meta carbon resonances in the β-phenyl group (C8,9,11,12) is demonstrated. Assignment of the quarternary carbon atoms, C2,7,13, can be achieved by optimizing the delays in the pulse sequence of the C–H correlation spectrum for small couplings[18] ("long-range couplings", Figure 2b). For the resonance at $\delta = 135.0$ ppm (assigned to C2), a cross peak is found to the ortho protons H8,12 which arises from ^{3}J coupling. The observation of a geminal coupling $^{2}J_{13C,1H}$ between C2 and H3 confirms this assignment. By analogy, $^{3}J_{13C,1H}$ coupling is observed between the signal at $\delta = 152.0$ ppm and the meta protons H9,11 which must therefore be the C7 resonance. The assignment of the remaining signal at 164.1 ppm to C13 is confirmed by an intense and by a weak cross peak with the corresponding meta (H15,17) and ortho (H14,18) protons, respectively.

As with the ^{1}H chemical shifts, the ^{13}C resonances of the ortho and para position C14,16,18 of the α-phenyl substituent appear at higher field than their counterparts C8,10,12, of the aromatic ring in β-position. In contrast, the ipso carbon resonance of C13 appears at lower field than the analogous ipso signal of C7 ($\Delta\delta = 12.1$ ppm). This probably also is due to the same effects which cause the resonance of C1 in **2** to appear at very low field.

^{6}Li NMR. A new 2D NMR method recently introduced by our group,[21,22] ^{6}Li–^{1}H–2D heteronuclear Overhauser effect spectroscopy (^{6}Li–^{1}H–2D HOESY),[38] allows the detection of short Li–H distances in solution based on dipolar relaxation effects. Applied to **2** (isotopically labeled with ^{6}Li) in THF-d_8, ^{6}Li–^{1}H HOESY reveals a very intense cross peak between the ^{6}Li singlet

(25) All ^{1}H NMR multiplicities are referred to spectral appearance rather than to exact subspectral analysis. The stated coupling constants are taken from the spectra according to first-order rules and are reported as the directly measured values; i.e., slight deviations between corresponding coupling constants may be present.

(26) Seebach, D.; Hässig, R.; Gabriel, J. *Helv. Chim. Acta* **1983**, *66*, 308. Seebach, D.; Gabriel, J.; Hässig, R. *Helv. Chim. Acta* **1984**, *67*, 1083.

(27) The correlation between coupling constants is $J_{13C,7Li} = (\gamma_{7Li}/\gamma_{6Li}) \cdot J_{13C,6Li} = 2.641 \cdot J_{13C,6Li}$.

(28) Fraenkel, G.; Fraenkel, A. M.; Geckle, M. J.; Schloss, F. J. *J. Am. Chem. Soc.* **1979**, *101*, 4745. Fraenkel, G.; Henrichs, M.; Hewitt, J. M.; Su, B. M.; Geckle, M. J. *J. Am. Chem. Soc.* **1980**, *102*, 3345.

(29) Fraenkel, G.; Hsu, H.; Su, B. M. In *Lithium, Current Applications in Science, Medicine, and Technology*; Bach, R. O., Ed.; J. Wiley: New York, 1985; p 273f.

(30) Breitmaier, E.; Voelter, W. *Carbon-13 NMR Spectroscopy*; VCH Publishers: Weinheim, FRG, 1987.

(31) Bauer, W.; Winchester, W. R.; Schleyer, P. v. R. *Organometallics* **1987**, *6*, 2371.

(32) Jackman, L. M.; Scarmoutzos, L. M. *J. Am. Chem. Soc.* **1984**, *106*, 4627.

(33) Jones, A. J.; Grant, D. M.; Russell, J. G.; Fraenkel, G. *J. Phys. Chem.* **1969**, *73*, 1624.

(34) Knorr, R.; von Roman, T.; von Roman, U., private communication. We thank Prof. Knorr, Munich, for providing us with unpublished data.

(35) Bauer, W.; Schleyer, P. v. R., unpublished results.

(36) Hogen-Esch, T. E. *Adv. Phys. Org. Chem.* **1977**, *15*, 154. Szwarc, M.; *Ions and Ion-Pairs in Organic Reactions*; Wiley: London, 1972; Vol. 1, 1974; Vol. 2.

(37) Freeman, R.; Morris, G. A. *Chem. Commun.* **1978**, 684.

(38) First description of ^{13}C–^{1}H–2D HOESY: Rinaldi, P. L. *J. Am. Chem. Soc.* **1983**, *105*, 5167. Yu, C.; Levy, G. C. *J. Am. Chem. Soc.* **1983**, *105*, 6994. Yu, C.; Levy, G. C. *J. Am. Chem. Soc.* **1984**, *106*, 6533.

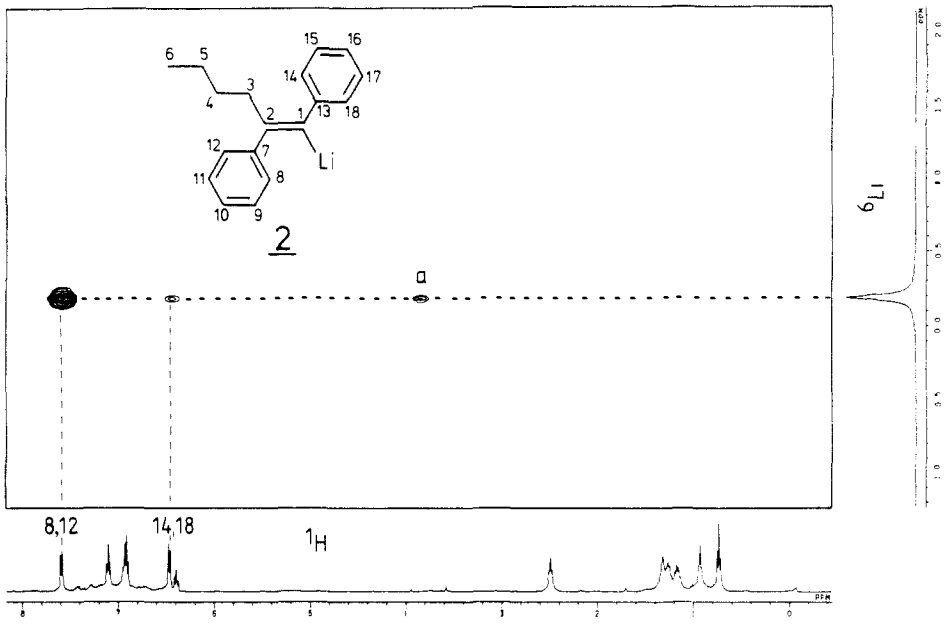

Figure 4. ^{6}Li–^{1}H–2D heteronuclear Overhauser spectroscopy (HOESY) of **2**, contour plot, THF-d_8, in situ preparation, 96% enriched with ^{6}Li, −30 °C, 0.7 M, mixing time[38] 2.5 s; a = axial signal at $f_1 = 0$ (cf. Figure 11 and ref 62).

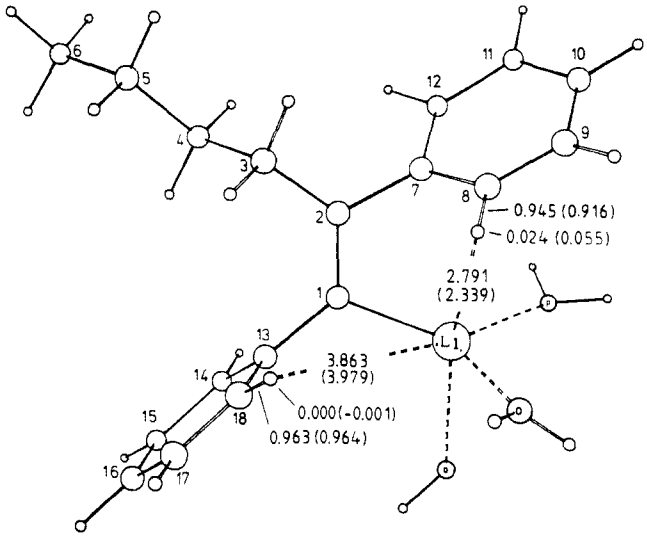

Figure 5. MNDO calculated structure of **2** with three water molecules as ligands. Bond lengths (Å) are shown at the dashed lines; values given at the hydrogen atoms are LUMO coefficients and values at the C–H bonds are bond orders. The numbers in parentheses are analogous values calculated with only two water molecules as ligands.

and the ^{1}H doublet assigned to H8,12 (Figure 4). A much weaker cross peak is observed between ^{6}Li and the second pair of ortho hydrogen atoms, H14,18. This finding secures the ^{1}H NMR assignments made on the basis of chemical shifts and examination of molecule models. Moreover, this provides further proof of the trans geometry of the *n*BuLi–tolane reaction product: a cis compound **7** should reveal ^{6}Li–^{1}H HOESY cross peaks including the ortho positions H14,18 and the allylic position H3, respectively, but this is not found experimentally.

MNDO Calculations. Semiempirical calculations (MNDO)[39] have been shown to reproduce and even to predict the general geometrical features of organolithium compounds shown by X-ray structures quite well (e.g., 2,6-bis(lithiotrimethylsilylmethyl)-pyridine·2TMEDA,[40] [3,6-di(lithio-THF)-2,2,7,7-tetramethyl-3,4,5)octatriene]$_2$,[41] and 1,3-dilithiodibenzylketone·2TMEDA).[42]

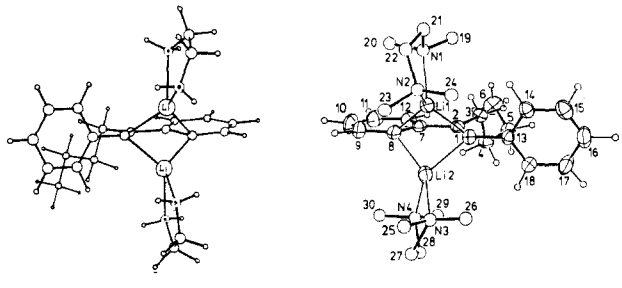

Figure 6. Right: molecular structure of (*E*)-1,8-dilithio-1,2-diphenyl-hex-1-ene **3**·2TMEDA (ORTEP plot; displacement ellipsoides at the 50% probability level; H atoms with arbitrary radii, TMEDA atoms with arbitrary radii without H atoms for clarity; only one alternative is shown for the disordered CH_2 group C27). Left: MNDO-calculated structure of **3**·2EDA (EDA = ethylenediamine) plotted enantiomeric to the X-ray structure; $\Delta H_f° = -44.9$ kcal/mol.

Figure 5 shows the MNDO-results for monomeric **2** calculated with three water molecules as model ligands for THF. The experimental findings shown in Figure 4 are corroborated nicely: lithium is in much closer proximity to the ortho hydrogen H8 than to H18. As was found in other examples (e.g., lithionaphthalene),[22] this is shown calculationally (MNDO) by a larger LUMO coefficient of the proton close to lithium and a reduced C–H bond order. Clearly, H8 is activated to a greater extent toward lithiation than H18. This difference is even greater when calculations are carried out with only two water ligands (Figure 5). In that case, H8 functions as a ligand for lithium. This is important with regard to the formation of the dilithio compound **3**, as is discussed in the next section.

Dilithioproduct 3. Preparation. The reaction of tolane with 1 equiv of *n*BuLi in THF at 0 °C leads only to the green monolithio product **2**. No further metalation is observed under these conditions. However, when the same reaction is carried out in the reaction medium first described by Mulvaney,[7] i.e., in hexane/TMEDA at 0 °C, a *red* reaction solution forms immediately. After addition of *1 equiv* of *n*BuLi, a finely divided yellow precipitate is formed after 1.5 h. This was observed by Mulvaney after addition of *2.5 equiv* of *n*BuLi.[7] After removal of the solvent (hexane) and dissolving both the precipitate and the residual oil in benzene-d_6, the ^{1}H and ^{13}C NMR spectra show the signals of

(39) Dewar, M. J. S.; Thiel, W. *J. Am. Chem. Soc.* **1977**, *99*, 4899, 4907.
(40) Hacker, R.; Schleyer, P. v. R.; Reber, G.; Müller, G.; Brandsma, L. *J. Organomet. Chem.* **1986**, *316*, C4.
(41) Neugebauer, W.; Geiger, G. A. P.; Kos, A. J.; Stezowski, J. J.; Schleyer, P. v. R. *Chem. Ber.* **1985**, *118*, 1504.
(42) Kos, A. J.; Clark, T.; Schleyer, P. v. R. *Angew. Chem., Int. Ed. Engl.* **1984**, *23*, 620. Dietrich, H.; Mahdi, W.; Wilhelm, D.; Clark, T.; Schleyer, P. v. R. *Angew. Chem., Int. Ed. Engl.* **1984**, *23*, 621.

Table III. ^{13}C, ^{6}Li Coupling Constants of Monomeric Vinyllithium Derivatives **16** in THF

	R¹	R²	R³	R⁴	R⁵	$J_{^{13}C,^{6}Li}$[a] (Hz)	temp (°C)	lit.
2	*n*Bu	Ph	H	H	H	10.6	−91	this work
16a	H	H	Me	H	H	12.0	−127	34
16b	H	H	Me	Me	Me	11.0	−113	34
16c	Me	Me	H	H	H	11.0	−126	34

[a] All observed multiplicities are 1:1:1 triplets.

Table IV. Important Bond Lengths (Å) and Angles (deg) for (*E*)-1,8-dilithio-1,2-diphenylhex-1-ene, **3**·2TMEDA[a]

Li1–C1	2.197 (8)	Li2–C1	2.19 (1)
Li1–C8	2.09 (1)	Li2–C8	2.158 (8)
Li1–C2	2.534 (8)	Li2–C2	2.694 (9)
Li1–C7	2.541 (9)	Li2–C7	2.653 (9)
Li1–N1	2.164 (8)	Li2–N3	2.167 (8)
Li1–N2	2.113 (9)	Li2–N4	2.174 (9)
C1–C2	1.353 (6)	C2–C3	1.532 (6)
C1–C13	1.476 (7)	C2–C7	1.516 (7)
C7–C8	1.436 (7)	C7–C12	1.417 (6)
C8–C9	1.406 (7)	C11–C12	1.400 (8)
C9–C10	1.384 (8)	C10–C11	1.388 (9)
Li1–Li2	2.63 (1)		
C1–Li1–C8	85.1 (3)	C1–Li2–C8	83.6 (3)
N1–Li1–N2	84.9 (3)	N3–Li2–N4	83.8 (3)
Li1–C1–Li2	73.8 (3)	Li1–C8–Li2	76.6 (3)
C13–C1–C2	120.1 (4)	C1–C2–C3	123.1 (4)
C1–C2–C7	120.1 (4)	C7–C2–C3	116.8 (4)
C2–C7–C8	119.0 (4)	C2–C7–C12	120.2 (4)

[a] Estimated standard deviations in units of the last significant figure are given in parentheses.

both the monolithio compound **2** and of a second species identified later as the dilithio compound **3**. When isolated from the reaction mixture, washed with hexane, and dissolved in benzene-d_6, the precipitate gives only NMR signals of this second species. When tolane is reacted with 2 equiv of *n*BuLi in hexane/TMEDA at 0 °C, an initially dark red solution is produced, and, after several hours at 0 °C, red crystals are formed. These were dark red because of their larger size but gave ^{1}H and ^{13}C NMR spectra identical with those of the precipitate described above.

X-ray and MNDO Structure. X-ray structure analysis shows **3**·2TMEDA to be the predicted[4] trans dilithio product (Figure 6). In the solid state, **3** is a monomer with a nearly symmetrically doubly lithium bridged structure similar to, e.g., dilithiobiphenyl (**17**),[43] dilithio diphenyl ether (**18**),[44,45] and the dilithiated *o*-xylene derivative **19**.[46] This doubly lithium bridging can be considered

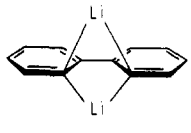

17

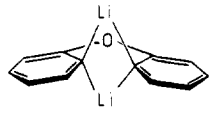

18

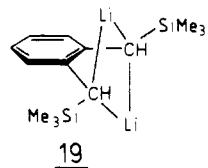

19

as the intramolecular equivalent of dimerization.[47] Each lithium atom is chelated with one TMEDA molecule and achieves a tetrahedral coordination sphere. Selected bond lengths and angles for **3**·2TMEDA are summarized in Table IV. The double bond C1–C2 is strictly planar (dihedral angle C13–C1–C2–C7 = 180.0°). The nonmetalated phenyl ring is almost perpendicular to the π-system involved in lithium bridging (dihedral angle C14–C13–C1–C2 = 100.8°). To the hydrocarbon framework of **3**, all Li–H distances are larger than 3.1 Å. However, closer contacts between Li and the hydrogen atoms of the TMEDA-methyl groups are found in the crystal. These contacts can also be detected in solution by NMR, as is discussed below.

Table V. ^{1}H NMR Chemical Shifts (δ, ppm), Multiplicities,[25] and Coupling Constants (Hz)[25] for Dissolved Crystals of **3**·2TMEDA in Benzene-d_6 (+21 °C) and THF-d_8 (−71 °C)[d]

H	**3**·2TMEDA, C_6D_6	**3**·2TMEDA, THF-d_8	**24**, THF-d_8
3	3.09, t, 8.3 Hz	2.46, m	2.37, m
4	2.10, m	1.53, m	1.46, m
5	1.63, hex, 7.2 Hz	1.28, m	1.16, m
6	1.11, t, 7.3 Hz	0.82, t, 7.2 Hz	0.74, t, 7.1 Hz
9	8.51, d, 5.5 Hz	7.94, d, 6.1 Hz	8.04, d, 6.6 Hz
10	7.41, t, 6.6 Hz	6.66, t, 6.6 Hz	6.85, t, 6.9 Hz
11	7.23, t, 7.2 Hz	6.84[a]	7.04, t, 7.6 Hz
12	7.98, d, 8.0 Hz	7.28, d, 7.8 Hz	7.45, d, 8.1 Hz
14	6.99 d, 6.8 Hz	6.52, d, 7.3 Hz	6.61[b]
15	7.54, t, 7.5 Hz	6.93, t, 7.6 Hz	7.06, t, 7.1 Hz[c]
16	7.03, t, 7.0 Hz	6.41, t, 7.2 Hz	6.60[b]
17	7.54, t, 7.5 Hz	6.93, t, 7.6 Hz	7.00, t, 7.7 Hz[c]
18	6.99, d, 6.8 Hz	6.52, d, 7.3 Hz	6.63[b]
TMEDA-CH_2	1.86, s	2.29, s	
TMEDA-CH_3	1.94, s	2.12, s	

[a] Hidden under triplet of H10 of **24**. [b] The chemical shifts of H14,16,18 in the dimer **24** are too similar for extraction of coupling constants. [c] Assignments may be interchanged. [d] 0.3 M; for numbering see formula in text and Figure 7.

MNDO calculations on **3**, carried out with two ethylenediamine (EDA) model ligands instead of TMEDA, are in remarkably good accord with the X-ray structure (Figure 6); the structure with nearly symmetrical doubly lithium bridging is the most stable. The most notable difference to the solid-state structure arises from different conformations of the *n*-butyl group, which is antiperiplanar in the MNDO calculations but gauche (−64.1°) in the crystal. This is almost certainly due to intermolecular (packing) forces, which are neglected in the calculations thus resulting in the expected trans arrangement.

Lithiation Mechanism. The addition of *n*BuLi to tolane and the second metalation are separate steps. By using a 1:1 ratio of *n*BuLi/tolane, the reaction in THF stops after the formation of the addition product **2**. However, in hexane/TMEDA the subsequent second metalation cannot be prevented. Therefore, we assume that in excess THF the lithium atom in **2** is coordinated by three THF ligands (Figure 5); hence the "activation" of H8 (the second H atom to be replaced) is small. However, in hexane/TMEDA, this activation evidently is much stronger. This probably is due to chelation of Li with only one TMEDA molecule. This leaves one coordination site open which can be occupied by the ortho hydrogen atom H8 in **2**. The MNDO structure of **2** calculated with two water ligands models this situation (Figure 5). This suggests that **2**·TMEDA already is activated toward second lithiation. This contrasts with the results obtained for 1-lithionaphthalene **14** where a mixed complex between the monolithio compound and the metalation reagent is necessary to function as the metalation-directing intermediate.[22]

^{1}H and ^{13}C NMR. Crystals of **3**·2TMEDA, when dissolved in benzene-d_6, give NMR spectra which show that the structure in the solid state is retained in solution. In the ^{1}H NMR spectrum, H9 (which is now in vicinity of a doubly lithium bridged carbon atom) appears at very low field (δ = 8.51 ppm; Table V) as a broadened doublet; its coupling constant ($^{3}J_{H9,H10}$ = 5.5 Hz) is smaller than "normal" values in aromatic systems ($^{3}J_{H,H}$ = ca. 7.5 Hz). This reduction is consistent with data for other lithiated aromatic compounds, e.g., 1-lithionaphthalene (**14**),[22] 2-lithiophenylpyrrole (**13**),[21] or 2-lithio-*tert*-butylphenylthioether **20**,[48] and is generally found in aromatic systems with electropositive substituents.[49] No separate resonances for the ortho and meta protons H14,18 and H15,17, respectively, of the nonlithiated aromatic ring are observed under these conditions. Hence, the

(43) Schubert, U.; Neugebauer, W.; Schleyer, P. v. R. *Chem. Commun.* **1982**, 1184.
(44) Neugebauer, W.; Dietrich, H.; Schleyer, P. v. R., unpublished results.
(45) Setzer, W.; Schleyer, P. v. R. *Adv. Organomet. Chem.* **1985**, *24*, 353.
(46) Lappert, M. F.; Raston, C. L.; Skelton, B. W.; White, A. H. *Chem. Commun.* **1982**, 14.
(47) Schleyer, P. v. R. *Pure Appl. Chem.* **1984**, *56*, 151.
(48) Bauer, W.; Klusener, P. A. A.; Harder, S.; Kanters, J. A.; Duisenberg, A. J. M.; Brandsma, L.; Schleyer, P. v. R. *Organometallics* **1988**, *7*, 552.
(49) Castellano, S.; Sun, C. *J. Am. Chem. Soc.* **1966**, *88*, 4741.

Table VI. ^{13}C NMR Chemical Shifts of Dissolved Crystals of 3·2TMEDA (Labeled with ^6Li) in Benzene-d_6 (+24 °C) and THF-d_8 (−71 °C)[e]

C	3·2TMEDA, C_6D_6	3·2TMEDA, THF-d_8	**24**, THF-d_8
1	202.0	202.1[a]	190.2[b]
2	145.2	144.7	150.8
3	31.6	32.0	32.9
4	34.7	35.0	34.4
5	24.3	24.9	24.6
6	14.4	15.0	14.9
7	154.2	154.8	154.9
8	189.0	189.5[c]	175.9[d]
9	143.7	143.7	143.4
10	122.3	121.9	123.3
11	125.4	124.9	126.6
12	122.4	121.7	124.3
13	163.1	163.8	161.3
14	122.0	121.7	123.3
15	127.8	127.8	128.2
16	117.2	116.6	119.3
17	127.8	127.8	128.2
18	122.0	121.7	123.0
TMEDA-CH_2	56.8	58.5	
TMEDA-CH_3	45.8	46.5	

[a] $J_{13C,6Li}$ = 5.9 Hz. [b] $J_{13C,6Li}$ = 4.1 Hz, 4.1 Hz, 7.7 Hz. [c] $J_{13C,6Li}$ = 7.6 Hz. [d] $J_{13C,6Li}$ = 4.3 Hz, 4.3 Hz, 6.1 Hz. [e] 0.4 M; for numbering see formula in text and in Figure 9.

barrier to rotation around the C1–C13 bond must be quite low. Strikingly, the TMEDA–methyl ^1H resonance appears at *lower* field than that of the TMEDA–methylene singlet.[50] This must be due to spatial proximity of these protons to the lithium atoms which produce a deshielding effect similar to that observed for the ortho protons H8,12 in **2** (Figure 1). Consequently, the TMEDA ligands must be tightly bound to lithium under these conditions. The same behavior was observed for 1-lithio-2,4,6-tri-*tert*-butylbenzene (**21**) ("supermesityllithium"–TMEDA): in

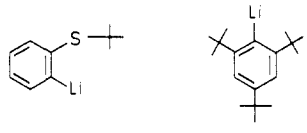

20 **21**

a benzene-d_6 solution of the crystals of **21**, the ^1H NMR signal of the TMEDA methyl groups appears downfield from that of CH_2, whereas in a THF-d_8 solution the order is reversed, indicating that TMEDA is "free" and is not functioning as a ligand.[31] This finding is corroborated by the ^6Li–^1H HOESY experiment described below.

The ^{13}C NMR spectrum of 3·2TMEDA in benzene-d_6 solution (Table VI) shows the resonance of C1 shifted upfield as compared to the monolithio precursor **2** ($\Delta\delta$ = −6.2 ppm). This parallels the findings for monomeric, dimeric, and tetrameric phenyllithium where the ^{13}C resonances for C1 of the aggregates appear at higher field than that of the monomer[31] and reflects the "intramolecular dimerization" by double lithium bridging in 3·2TMEDA in benzene-d_6 solution. Since the resonance of the lithiated aromatic carbon atom C8 in 3·2TMEDA appears at δ = 189.0 ppm, exactly the value found for *dimeric* phenyllithium,[26] the bonding situations are indicated to be quite similar.

Very unusual results are obtained when the dark red crystals of 3·2TMEDA are dissolved in THF-d_8 to give a *green* solution. The ^1H and ^{13}C NMR spectra now show a temperature and concentration dependent equilibrium between *two* species. At −71 °C in 0.3 M THF-d_8 solution, the ^1H NMR signals for these two species have a 3.6:1 intensity ratio. With increasing temperature and at lower concentrations, the intensity of the major compound, characterized by a low field ^1H NMR doublet at δ = 8.04 ppm,

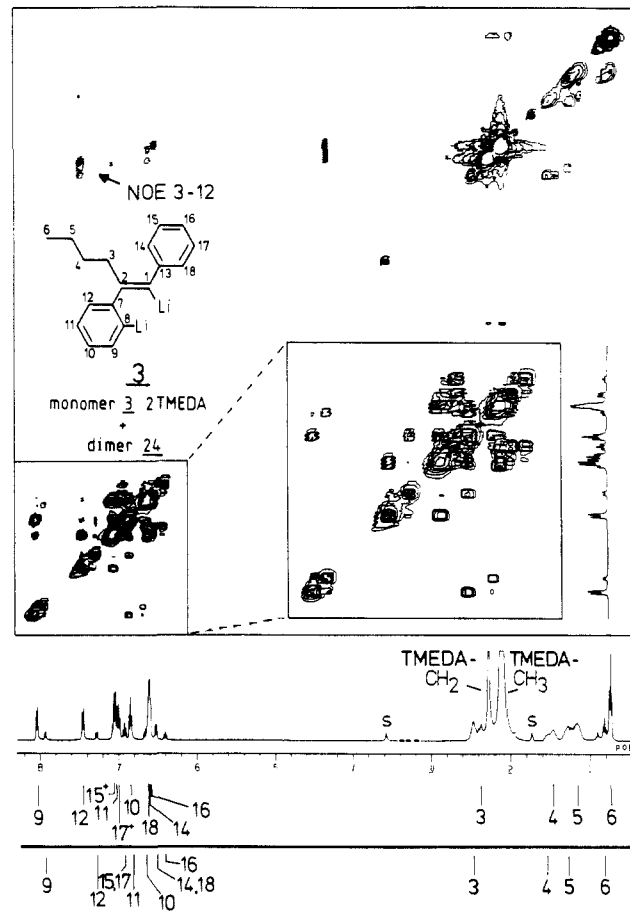

Figure 7. ^1H–^1H COSY (below diagonal) and NOESY (above diagonal) of dissolved crystals of 3·2TMEDA; combined COSY–NOESY pulse sequence ("COCONOESY"),[15] THF-d_8, 0.3 M, −71 °C, mixing time 700 ms with statistical ±5% variation; s = solvent; assignment below one-dimensional spectrum: upper row: major compound **24**; lower row: minor compound 3·2TMEDA; + = assignments may be interchanged.

increases. The connectivities of the coupled protons can be determined from the COSY plot (Figure 7). Both sets of data are compatible with structure **3**; i.e., no change of the constitution of **3** can have occurred during solution in THF. The ^1H chemical shifts in the aromatic region of the major compound appear at lower field than those of the minor species. Whereas the major compound shows slow rotation of the nonlithiated aromatic ring (four separate signals for H14,15,17,18), the barrier to rotation in the minor compound is low even at −71 °C (isochronicity of corresponding ortho and the meta protons). On warming to +25 °C, the separate signals for H14,18 and H15,17 of the major compound coalesce. A crude estimation using eq 3[51] gives an Eyring[52] free activation energy $\Delta G^{\ddagger}_{298}$ of 15.2 kcal/mol for this dynamic process.

$$k_{\text{coalescence}} = \frac{\pi\Delta\nu}{\sqrt{2}} \qquad (3)$$

Assuming that the minor species in Figure 7 is identical with the structure shown by X-ray and NMR data in benzene solution (as demonstrated below), several possibilities can be considered for the major compound, e.g., (i) a cis isomer **22** where the lithium

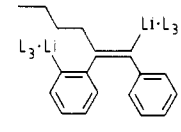

22

L = THF-d_8 or η^1-TMEDA

(50) In a binary TMEDA–benzene-d_6 mixture, this order is reversed, and the methylene protons appear downfield from the methyl resonance.

(51) Gutowsky, H. S.; Holm, C. H. *J. Chem. Phys.* **1956**, *25*, 1228.
(52) Eyring, H. *Chem. Rev.* **1935**, *17*, 65.

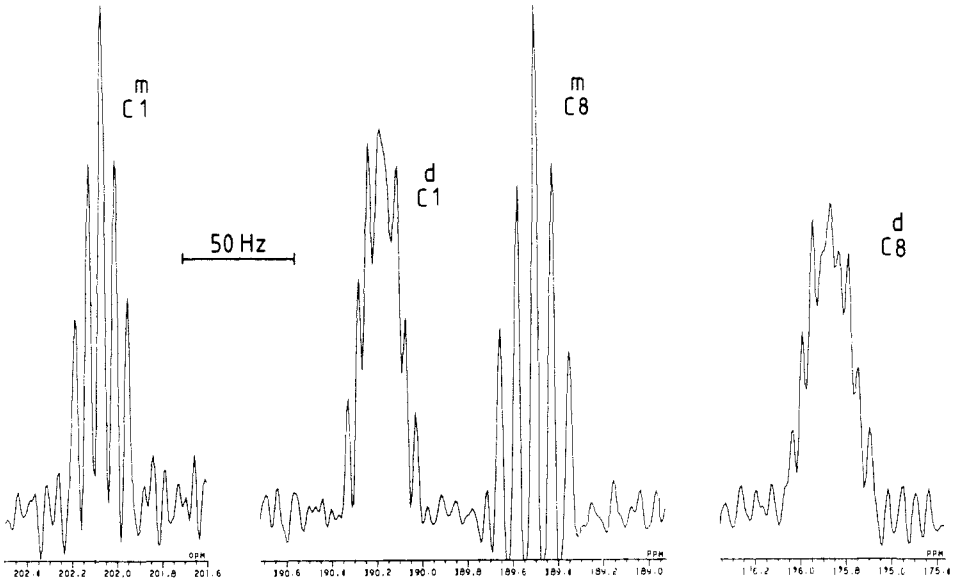

Figure 8. ^{13}C NMR signals of the lithiated carbon atoms of **3**·2TMEDA and **24** with resolution enhancement (Gauss filter); dissolved crystals of **3**·2TMEDA, enriched with ^{6}Li, THD-d_8, 0.3 M, −71 °C; indices m (monomer **3**·2TMEDA); d (dimer **24**).

double briding is disrupted and each lithium atom must be assumed to be threefold-coordinated by THF-d_8 or by TMEDA and (ii) a "head-to-head, tail-to-tail" dimer **23**. This is a somewhat

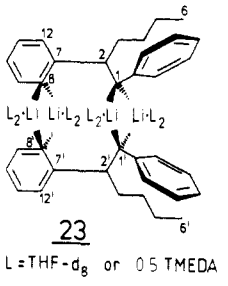

23

L = THF-d_8 or 0.5 TMEDA

curious structure, but a strain-free molecule model can be constructed. The central C1–C2–C7–C8–Li_2–C_8′–C7′–C2′–C1′–Li_2 ring can invert easily in a cyclohexane-like fashion. Neglecting the conformations of the *n*-butyl residues and the rotational positions of the nonlithiated aromatic rings, this inversion interchanges structures with C_2 and C_s symmetry. (iii) A dimer **24**

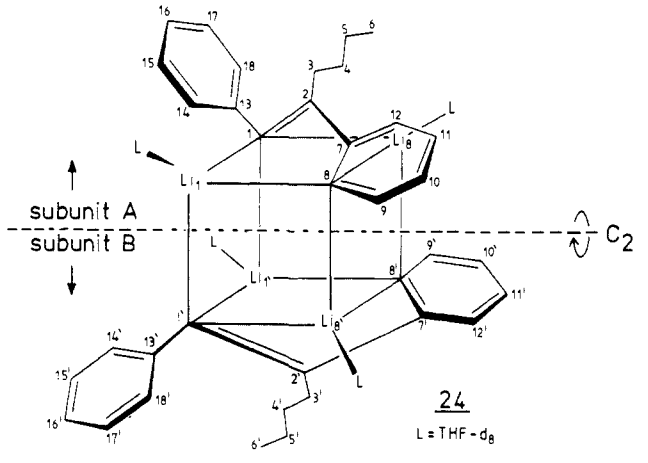

24

L = THF-d_8

based on the crystal state structure (Figure 6) with a central C_4Li_4 cubic arrangement analogous to that in tetrameric phenyllithium[53] (the TMEDA ligands are replaced by THF-d_8). This chiral species has C_2 symmetry, but due to intra- and interaggregate exchange, a racemic mixture would be present.

A distinction between structures **22**, **23**, and **24** could be made by determining the ^{13}C NMR spectrum of a THF-d_8 solution of crystals of **3**·2TMEDA which are isotopically enriched with ^{6}Li (spin $I = 1$). At −71 °C, quintets with intensity ratios 1:2:3:2:1 appear (Figure 8) for the metalated carbon atoms at $\delta = 202.1$ and at 189.5 ppm ($J = 5.9$ and 7.6 Hz, respectively). As these chemical shifts are identical with those already obtained for the single species in benzene-d_6 solution, the monomeric dilithio compound, **3**·2TMEDA, is implicated. The 5-fold splitting of each of the two signals indicates that the doubly lithium bridged structure is still present in THF-d_8 solution. As will be shown later, under these conditions even the TMEDA ligands are still chelated to the lithium atoms in this species. The other two ^{13}C resonances in Figure 8 show an unusual (and initially quite confusing) splitting pattern that seems not to have been observed before for analogous cases. In structure **22** each metalated carbon atom should show a 1:1:1 triplet in the ^{13}C NMR spectrum due to coupling with only one ^{6}Li atom. Clearly, this is not found experimentally. On the other hand, the line shapes of the signals at $\delta = 190.2$ and 175.9 ppm, respectively, are incompatible with coupling of ^{13}C only to *chemically equivalent* lithium atoms. This rules out a "head-to-head, tail-to-tail" dimer **23**, which should reveal ^{13}C NMR signals with "normal" 1:2:3:2:1 splitting. However, in dimer **24**, each of the carbon atoms C1, C1′, C8, and C8′ (which are pairwise chemically equivalent due to C_2 symmetry) is directly bonded to three lithium atoms, two of these are *equivalent* and *one different*. Thus, assuming that the coupling constant between ^{13}C and the fourth, remote ^{6}Li atom is essentially zero,[26] an A_2MX spin system is expected (X represents the ^{13}C nucleus and A,M the chemically nonequivalent ^{6}Li nuclei). Since $\Delta\nu_{AM}$, $\Delta\nu_{AX}$, $\Delta\nu_{MX} \gg J_{AM}$, J_{AX}, J_{MX}, first-order rules can be applied. Consequently, each ^{13}C signal consists of a 1:2:3:2:1 quintet further split by a 1:1:1 triplet with a differing coupling constant; this splitting pattern explains the observed line shapes.

The existence of dimer **24** under these conditions shows that an organolithium compound, *monomeric* in the crystalline state as well as in benzene-d_6 solution, actually is aggregated to a *higher extent* in THF. This is in contrast to all earlier findings where THF tends to *de*aggregate lithium clusters.[9,31,54] The reasons for this behavior will be clarified below. As expected for dimers, the ^{13}C chemical shifts for C1 and C8 in **24** appear upfield from those of the monomer **3**·2TMEDA ($\Delta\delta = 11.9$ and 13.6 ppm, respectively). Both C1 and C8 are bonded to three lithium atoms, a situation found in aryl- or vinyllithium *tetramers*. Indeed, C8 in dimer **24** resonates at $\delta = 175.9$ ppm which is almost exactly the same value found for C1 in *tetrameric* phenyllithium ($\delta = 176.2$ ppm).[32] The chemical shift of C1 in **24** ($\delta = 190.2$ ppm)

(53) Hope, H.; Power, P. P. *J. Am. Chem. Soc.* **1983**, *105*, 5320.

(54) Bauer, W.; Seebach, D. *Helv. Chim. Acta* **1984**, *67*, 1972.

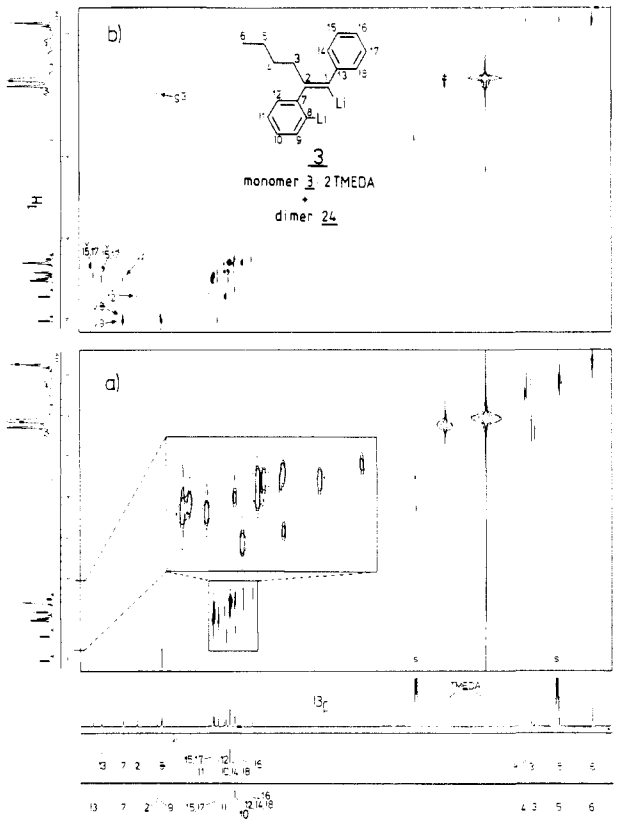

Figure 9. ^{13}C–^{1}H shift correlation spectroscopy, dissolved crystals of **3**·2TMEDA, THF-d_8, 0.3 M, −71 °C; assignment below one-dimensional ^{13}C spectrum: upper row = dimer **24**, lower row = monomer **3**·2TMEDA; s = solvent. (a) C–H shift correlation with delays in the pulse sequence set for direct couplings ($^{1}J_{13C,1H}$). (b) COLOC spectrum,[56] indicating long-range ^{13}C,^{1}H couplings and some of the direct couplings from spectrum (a). g = geminal coupling ($^{2}J_{13C,1H}$), v = vicinal coupling ($^{3}J_{13C,1H}$); numbers at cross peaks indicate hydrogen bonding partners.

is comparable with *tetrameric* vinyllithium in THF-d_8 at −86 °C: the C1 signals of dimeric and tetrameric vinyllithium appear at δ = 192.1 and 184.2 ppm, respectively.[35,55] For comparison, appropriate corrections for substitution have to be made (cf. ethylene, δ = 123.5 ppm; (*E*)-stilbene, $\delta_{\alpha\text{-}C}$ = 129.0 ppm).[30]

The assignments of the ^{13}C NMR resonances for both the monomer **3**·2TMEDA and the dimer **24** in THF-d_8, achieved by C–H shift correlation spectroscopy (Figure 9), are summarized in Table VI. The chemical shifts of the monomer **3**·2TMEDA in THF-d_8 at −71 °C are essentially identical with those found for the single species in benzene-d_6 solution at room temperature (Table VI). As already observed in the ^{1}H NMR spectrum, the ortho ^{13}C resonances (C14,18) appear as separate peaks for the dimer **24**, whereas for the monomer **3**·2TMEDA only one signal is found due to a low barrier to rotation around the C1–C13 bond.

The assignments of the quaternary carbon signals C2,C7 and C13 in **24** and in **3**·2TMEDA were achieved by the COLOC (correlation via long-range couplings) pulse sequence[56] which permits the detection of small ^{13}C–^{1}H couplings (usually $^{2}J_{13C,1H}$ and $^{3}J_{13C,1H}$). This method is superior in several respects to C–H shift correlation spectroscopy with delays optimized for long-range couplings. The cross peaks indicated in Figure 9b thus identify the quaternary ^{13}C atoms (Table VI).

(55) We question the explanation given in ref 29 that a "second resonance" found exactly at the same chemical shift as the vinyllithium tetramer (δ = 186.3 ppm) is due to a dimer. Rather, from natural abundance $^{6}Li/^{7}Li$ isotope distribution, the isotopomer abundance where one carbon atom is coupled to only *two* ^{7}Li nuclei is about 20% which might explain the observed splitting. Moreover, the coupling constants $J_{13C,7Li}$ of the "two species" seem to be identical.

(56) Kessler, H.; Griesinger, C.; Zarbock, J.; Loosli, H. R. *J. Magn. Reson.* **1984**, *57*, 331. Kessler, H.; Griesinger, C.; Lautz, J. *Angew. Chem., Int. Ed. Engl.* **1984**, *23*, 444.

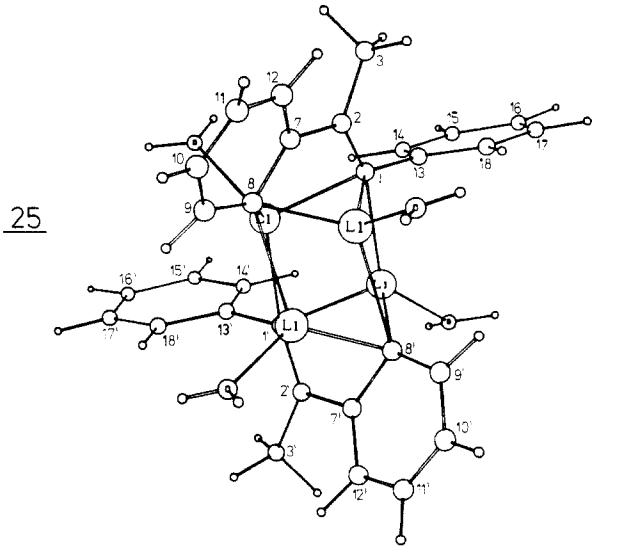

Figure 10. MNDO structure **25** of a simplified model of the dimer **24** (*n*-butyl replaced by methyl, THF-d_8 replaced by water) view along the "C_2 axis" (see text); $\Delta H_f°$ = −270.7 kcal/mol; the numbering is analogous to **24**; i.e., numbers 4, 5, and 6 do not appear in the methyl compound **25**.

MNDO Calculations. The dimer **24** was calculated by using MNDO with methyl groups instead of *n*-butyl and with four water molecules instead of THF as ligands: structure **25** shown in Figure 10 resulted.

Structure **25** was calculated both without any symmetry and with C_2 symmetry imposed, but nearly identical geometries resulted. The nonsymmetrical structure **25** in Figure 10 is somewhat more stable ($\Delta\Delta H_f°$ = −4.7 kcal/mol) than the C_2 form. The representation of **25** in Figure 10 is related to that of **24** turned 90° clockwise around a vertical axis. The distortion of the central C_4Li_4 moiety in **25** is similar to that found in tetrameric phenyllithium.[53] A molecular model of **25** reveals large steric hindrance to rotation for the nonlithiated phenyl rings. The barrier to rotation was estimated by calculating **25** with one ring fixed with a 90° twist angle and reoptimizing the structure. This gave an extremely high barrier, $\Delta E^{\ddagger}_{rot}$ = 42.2 kcal/mol. Even if $\Delta S^{\ddagger}_{rot}$ for this process would be abnormally high, this value does not agree with the experimental value, $\Delta G^{\ddagger}$ = 15.2 kcal/mol, for the exchange of the ortho and meta protons H14,15,17,18 in **24**. However, as will be explained in more detail below, the observed exchange does not take place in the *intact* dimer **24** (as assumed in the calculation) but by prior dissociation to the monomer. For comparison, the monomer **3**·2EDA (Figure 6 left) first was recalculated with a methyl instead of the *n*-butyl substituent; this gave $\Delta H_f°$ = −32.7 kcal/mol for the MNDO-optimized structure **26**. Calculation of the barrier to rotation of the nonlithiated aromatic ring in **26** (in analogy to the calculation for the dimer **25** described above) gave a drastically lower value of only $\Delta E^{\ddagger}_{rot}$ = 8.0 kcal/mol. This low barrier is consistent with the coalescence of the ^{1}H and ^{13}C NMR signals for positions 14,18 and for 15,17 of the monomer **3**·2TMEDA even at −71 °C.

^{6}Li NMR. The ^{6}Li NMR spectrum of crystals of **3**·2TMEDA dissolved in THF-d_8 under conditions of slow intra- and interaggregate exchange is expected to give three signals for the two species, monomer **3**·2TMEDA and dimer **24**. In **3** the two doubly bridging lithium atoms are chemically equivalent and therefore isochronous, but there are two different types of chemically nonequivalent lithium atoms in the dimer **24**: two Li atoms bridge C8 and C8′ and two different Li atoms bridge C1 and C1′. The experimental results (Figure 11) agree: two signals of equal intensity at δ = 1.21 and 0.52 ppm and a smaller signal at 0.73 ppm are found. The two "outer" signals must correspond to the dimer **24**, whereas the "inner" signal is due to the monomer **3**·2TMEDA. This is proven by the behavior when the temperature is varied: identical changes in intensity are exhibited by the outer signals. Fraenkel[57] first described an organolithium compound

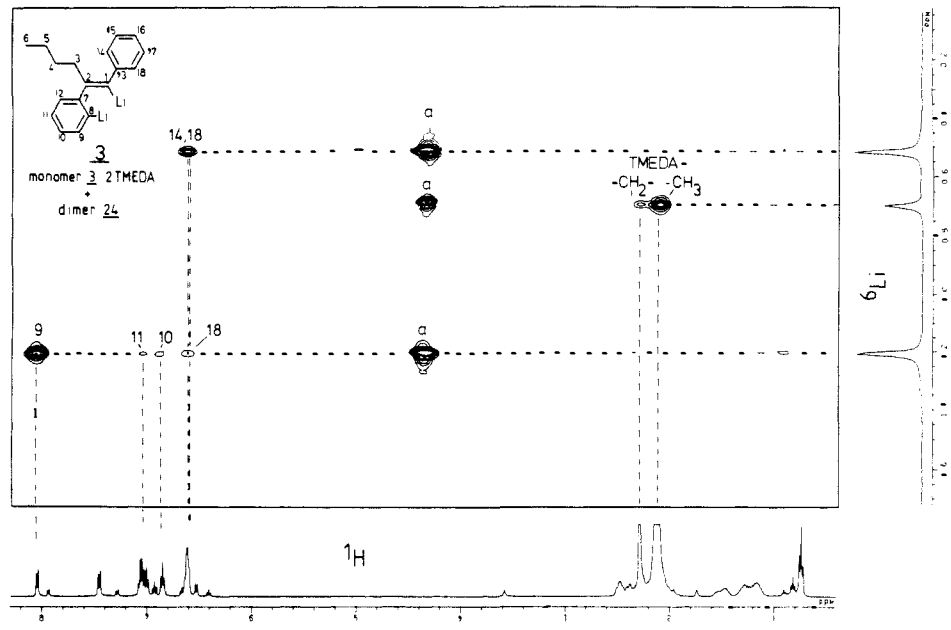

Figure 11. ^{6}Li–^{1}H HOESY, contour plot of **3**·2TMEDA and **24**, dissolved crystals of **3**·2TMEDA, THF-d_8, 0.3 M, 96% enriched with ^{6}Li, −71 °C, mixing time[38] 1.8 s; a = axial signal at f_1 = 0;[62] numbers at cross peaks indicate hydrogen positions involved in heteronuclear Overhauser enhancements.

which shows more than one Li signal due to anisochronicity. A recent example is given by Günther.[58]

Until now, ^{6}Li–^{1}H–2D HOESY[21,22,59] has been used for the detection of lithium–hydrogen interactions only involving a single lithium resonance. We describe here the first application of this technique for the assignment of *different* ^{6}Li signals. In the ^{6}Li–^{1}H HOESY spectrum of crystals of **3**·2TMEDA dissolved in THF-d_8 (Figure 11), the "inner" ^{6}Li signal of the monomer **3** at 0.73 ppm exhibits an intense cross peak to the TMEDA–CH_3 protons. Hence, TMEDA amust be attached to the lithium atoms of the monomer. No further cross peaks to hydrogen atoms of the monomer **3** are found, indicating that all of these positions must be remote from lithium. Indeed, the X-ray data (Figure 6) show the Li–H contacts to be closest for the TMEDA ligand (the smallest Li–CH_3 distance is 2.89 Å), whereas the closest contact between a hydrogen position of the monomer **3** and lithium is 3.14 Å (H14 in Figure 6). Other lithium–hydrogen distances in the X-ray structure (Figure 6) are much larger (>3.7 Å).

The two "outer" ^{6}Li signals of the dimer **24** are quite different and show no cross peak to TMEDA. This behavior is consistent with the geometry of **24**: each lithium in a corner of the C_4Li_4 moiety has only one coordination site available. This does not allow TMEDA to *chelate* lithium in a bidentate fashion. Obviously, under these conditions THF-d_8 is a better monohapto ligand than TMEDA. The low field ^{6}Li signal at δ = 1.21 ppm in Figure 11 has a very intense cross peak to the H9 doublet and is therefore assigned to Li8 in **24**. This is consistent with the Li8–H9 distance calculated (MNDO) for **25** in Figure 10. Further but much weaker cross peaks for the 1.21 ppm ^{6}Li signal are found to the remote H10 and H18 positions (the latter is the "peripheral" ortho hydrogen atom of a nonlithiated aromatic ring in **24**).[60] This observation also is consistent with the geometries indicated by MNDO and by molecular models. In contrast, the lithium signal at highest field (0.52 ppm) shows a single intense cross peak which

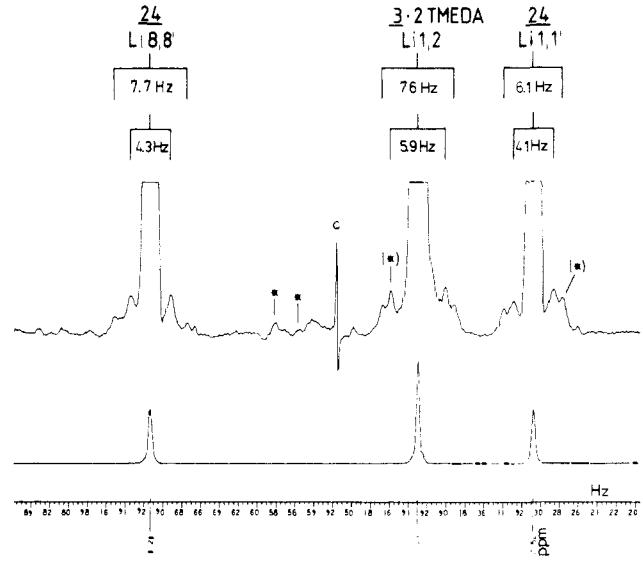

Figure 12. ^{6}Li NMR, crystals of **3**·2TMEDA dissolved in THF-d_8, 0.4 M, −71 °C, spinning speed 15 Hz; above: magnified spectrum with indicated ^{6}Li–^{13}C satellites; slight resolution enhancement (Gauss filter) was applied; c = carrier frequency spike. Visible and hidden spinning sidebands are marked * and (*), respectively. The accuracy of the satellite assignments was checked by several measurements by using different spinning speeds.

includes H14 and H18 (the resonances of these two protons are too close to be resolved in the f_1 domain of the 2D HOESY contour plot in Figure 11). Therefore, this ^{6}Li signal is assigned to Li1 in **24**. Again, this can be rationalized by means of MNDO and molecular models. The chemical shift order for the lithium atoms in the aryl (Li8) and in the vinyl (Li1) positions is consistent with the known ^{7}Li chemical shifts for phenyllithium (δ = 1.03 ppm) and for vinyllithium (more upfield, δ = 0.08 ppm) in diethyl ether.[61]

These assignments of the ^{6}Li signals for **3**·2TMEDA and **24** can be confirmed by using a different technique: by magnifying the one-dimensional ^{6}Li spectrum of Figure 11 greatly, the small satellites due to coupling of ^{6}Li with ^{13}C (1.1% abundance) can

(57) Fraenkel, G.; Hallden-Abberton, M. P. *J. Am. Chem. Soc.* **1981**, *103*, 5657.

(58) Günther, H.; Moskau, D.; Dujardin, R.; Maerker, A. *Tetrahedron Lett.* **1986**, *27*, 2251. Moskau, D.; Brauers, F.; Günther, H.; Maercker, A. *J. Am. Chem. Soc.* **1987**, *109*, 5532.

(59) Detection of short Li–H distances by one-dimensional ^{6}Li–^{1}H NOE spectroscopy is reported by the following: Avent, A. G.; Eaborn, C.; El-Kheli, M. N. A.; Molla, M. E.; Smith, J. D.; Sullivan, A. C. *J. Am. Chem. Soc.* **1986**, *108*, 3854.

(60) The very weak cross peak in Figure 11 between Li8 and H11 might arise from indirect NOE due to spin diffusion: Kövér, K.; Batta, G. *J. Magn. Reson.* **1986**, *69*, 519. Olejniczak, E. T.; Gampe, R. T., Jr.; Fesik, S. W. *J. Magn. Reson.* **1986**, *67*, 28.

(61) Scherr, P. A.; Hogan, R. J.; Oliver, J. P. *J. Am. Chem. Soc.* **1974**, *96*, 6055. The sign of the chemical shift values given in this paper is opposite to the now accepted convention of assigning positive numbers to downfield shifts, cf., *Pure Appl. Chem.* **1976**, *45*, 217.

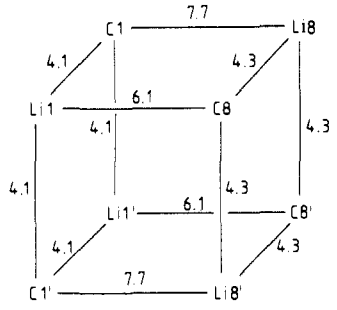

Figure 13. Central C_4Li_4 moiety of the dimer **24** showing the $^{13}C,^{6}Li$ coupling constants (Hz) deduced from the satellite peaks in Figure 12.

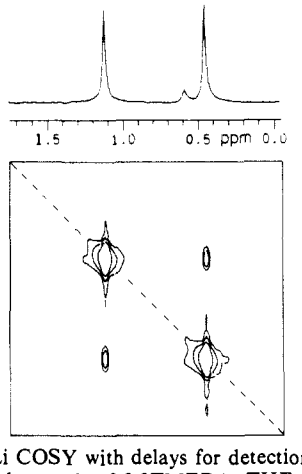

Figure 14. ^{6}Li–^{6}Li COSY with delays for detection of small coupling constants; dissolved crystals of **3**·2TMEDA, THF-d_8, −20 °C, 0.2 M, delays[18,58] $\Delta 1 = \Delta 2 = 400$ms, contour plot of nonsymmetrized absolute value spectrum.

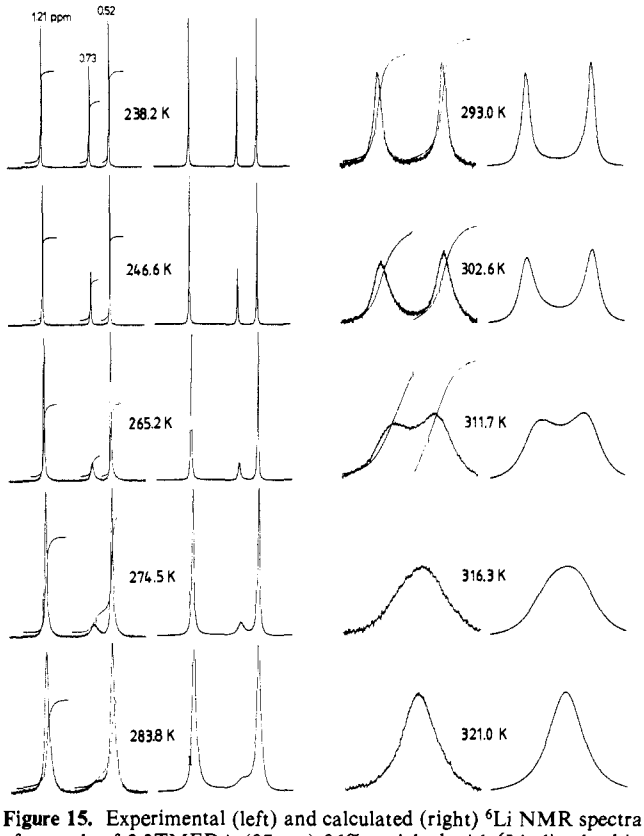

Figure 15. Experimental (left) and calculated (right) ^{6}Li NMR spectra of crystals of **3**·2TMEDA (97 mg) 96% enriched with ^{6}Li, dissolved in 0.45 mL of THF-d_8, relaxation delay 20 s. For frequency scales in ppm and hertz units, see Figures 11 and 12, respectively.

be observed (Figure 12). In the ^{13}C NMR spectrum (Figure 8), the two signals for C1 and C8 due to the monomer **3**·2TMEDA

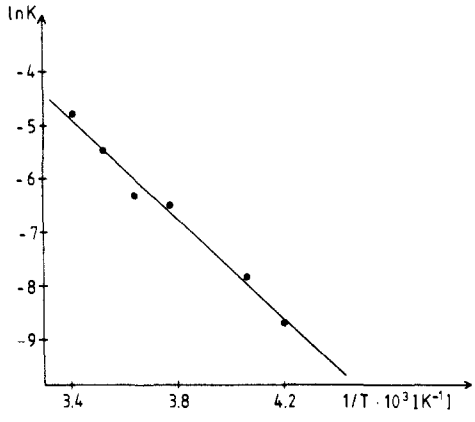

Figure 16. Van't Hoff plot (ln K versus $1/T$) for the equilibrium constants derived from eq 4 and from the spectra in Figure 15.

are split due to coupling with ^{6}Li ($J_{^{13}C,^{6}Li} = 5.9$ Hz and 7.6 Hz, respectively). Consequently, these couplings also must appear in the ^{6}Li spectrum. Indeed, the ^{6}Li signal assigned to monomer **3** reveals satellites with exactly these coupling constants. The two ^{6}Li signals of the dimer **24** show different behavior, whereas the high field resonance at $\delta = 0.52$ ppm, assigned to Li1 in **24** has two pairs of satellites with $J = 4.1$ Hz and $J = 6.1$ Hz (intensity ratio 2:1), the low field signal at 1.21 ppm, assigned to Li8, shows two pairs of satellites with $J = 4.3$ Hz and 7.7 Hz, respectively, also in a 2:1 intensity ratio. Thus, the ^{13}C–^{6}Li coupling situation in the dimer **24** must be as depicted in Figure 13. This again explains the unusual ^{13}C NMR signals found for the dimer **24** in Figure 8.

The magnitudes of the averaged $^{13}C,^{6}Li$ coupling constants for dilithio *dimer* **24** correspond more closely to values generally associated with organolithium *tetramers*,[31] where the bonding situation is similar to that shown in Figure 13.

A recently reported 2D NMR method, ^{6}Li–^{6}Li COSY with delays for the detection of small couplings[58] (applied to 3,4-dilithio-2,5-dimethyl-2,4-hexadiene), confirms the finding that the two ^{6}Li NMR signals at $\delta = 1.21$ and 0.52 ppm are due to a single species. In principle, there should be finite scalar coupling between the unisochronous lithium atoms Li1,1′ and Li8,8′ in **24**. However, the one-dimensional ^{6}Li spectrum of **24** (Figure 11) reveals sharp singlets ($\Delta\nu_{1/2} \approx 1$ Hz), i.e., the ^{6}Li–^{6}Li coupling constants in **24** must be even smaller. Similar results were obtained earlier by Brown,[63] who failed to detect any ^{6}Li–^{7}Li coupling in methyllithium aggregates.

COSY with fixed delays[18] permits the detection of small couplings that may be unresolved in one-dimensional spectra due to the width of the signals. Indeed, applied to a dimer **24**/monomer **3**·2TMEDA–THF-d_8 mixture, this method reveals cross peaks between the ^{6}Li signals of the dimer, due to scalar coupling (Figure 14). This proves that the corresponding signals are due to the same molecule.

Thermodynamics and Kinetics. Why is **3** aggregated to a greater extent in THF than in benzene or in the crystal state? Upon dissolving crystals of **3**·2TMEDA in THF, an equilibrium 4 can

$$\underset{\text{monomer}}{2(\mathbf{3}\cdot 2\text{TMEDA})} + 4\text{THF} \rightleftharpoons \underset{\text{dimer}}{\mathbf{24}} + 4\text{TMEDA} \qquad (4)$$

be assumed. For quantitative extraction of both thermodynamic

(62) Additional intense contours in Figure 11 (designated by "a") appear in the center of the ^{1}H spectrum (f_1 domain) at the positions of the Li signals. Due to quadrature detection in the t_1 domain, this position is $f_1 = 0$. The "axial peaks" a are due to spin–lattice relaxation during the t_1 period in the HOESY pulse sequence and reflect z-magnetization unlabeled by the proton chemical shifts (cf. Bax, A. *Two-Dimensional NMR in Liquids*; Reidel: Boston, 1982; p 19). For the 2D plot shown in Figure 11, we applied the pulse sequence described by Levy[38] which uses a 16-step phase cycle. The residual axial peaks in Figure 11 can be suppressed by 90° phase incrementation of the 180° ^{6}Li pulse every 16 scans which gives a 64-step phase cycle. Further spectral artifacts can be eliminated by application of four-step CYCLOPS.

(63) Brown, T. L.; Seitz, L. M.; Kimura, B. Y. *J. Am. Chem. Soc.* **1968**, *90*, 3245.

Scheme II

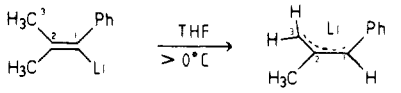

10 11

and kinetic data of the equilibrium in eq 4, a series of temperature dependent ^{6}Li NMR spectra of THF-d_8 dissolved crystals of **3**·2TMEDA was recorded and subjected to line-shape analysis (Figure 15). Integration of the ^{6}Li signals gives the relative concentrations of the monomer **3**·2TMEDA and of the dimer **24**. On the basis of the equilibrium in eq 4[64] and the van't Hoff plot in Figure 16, the thermodynamic parameters $\Delta H° = 9.4 \pm 0.6$ kcal/mol and $\Delta S° = 22.2 \pm 2.1$ eu are deduced. The dimerization reaction (eq 4) is endothermic. This is due to loss of the Li–TMEDA chelation energy. The positive entropy (despite the presence of one less particle on the right side of eq 4) results from the entropy gain due to free rotation in the nonchelating TMEDA molecules.

For quantitative modelling of the experimental value for $\Delta H°$, eq 5 was calculated with MNDO. As was the case in Figure 10, the *n*-butyl group is replaced by methyl, THF is simulated by water, and TMEDA is represented by ethylenediamine (EDA). The MNDO $\Delta H_f°$ values[65] in kcal/mol are given in eq 5. For

$$\underset{2\cdot(-32.7)}{2\cdot\mathbf{26}} + \underset{4\cdot(-60.9)}{4H_2O} \rightleftharpoons \underset{-270.7}{\mathbf{25}} + \underset{4\cdot(-5.7)}{4EDA} \qquad (5)$$

$$\Delta H_f° = 15.5 \text{ kcal/mol}$$

equilibrium 5 $\Delta H_f°$(calcd) = 15.5 kcal/mol was obtained. This is of the same magnitude as the experimentally found $\Delta H_f°$(exp) = 9.4 kcal/mol for eq 4.[66]

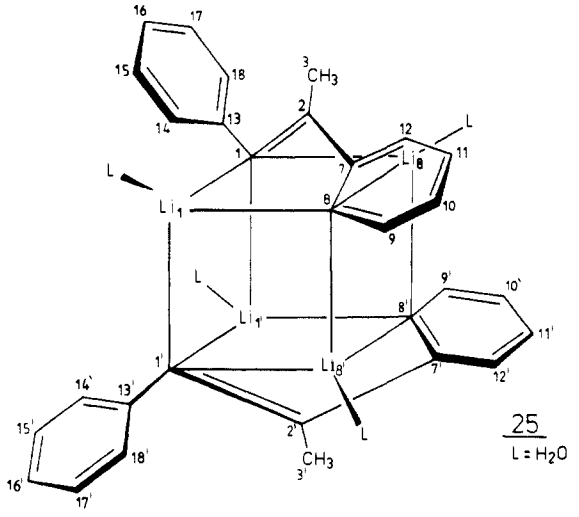

25 L = H_2O

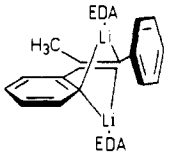

26

Activation parameters for the NMR behavior shown in Figure 15 were evaluated from line shape analysis. Two dynamic processes have to be considered: exchange between monomer **3**·2TMEDA and dimer **24** (eq 4) and exchange of the Li positions *within* dimer **24**. Thus, the situation is summarized by Scheme III, where A is the ^{6}Li nuclei in the monomer **3**·2TMEDA and B,C represent the chemically nonequivalent Li positions in the dimer **24**. Since in both the monomer **3**·2TMEDA and in the dimer **24** isochronous pairs of Li atoms are present and no significant scalar coupling between them is observed, Scheme III may be simplified to Scheme IV.

Scheme III

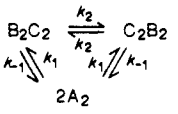

Scheme IV

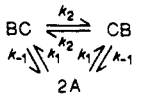

Table VII. Line Shape Analysis Data for the Spectra in Figure 15[a]

T [K]	$1/T\cdot10^3$	c_{rel} = [BC]/[A]^2 [(l/mol)]	k_1^{NMR} [s^{-1}]	k_{-1} [s^{-1}]	k_2 [s^{-1}]
208.3	4.801	1.07	(<0.1)		(<0.1)
238.2	4.198	1.50	(<0.1)		(<0.1)
246.6	4.055	2.03	0.4	0.197 ± 0.1	(<0.1)
265.2	3.771	3.45	2.0	0.580 ± 0.2	0.5 ± 0.2
274.5	3.643	3.70	6.0	1.622 ± 0.4	1.5 ± 0.3
283.8	3.542	5.26	12.0	2.281 ± 1.0	5.5 ± 1.0
293.0	3.413	7.14	45.0	4.504 ± 3.0	12.0 ± 2.0
302.6	3.305	12.50	75.0	7.508 ± 2.5	25.0 ± 4.0
311.7	3.208		90.0		64.0 ± 6.0
316.3	3.162		110.0		97.0 ± 8.0
321.0	3.115		130.0		137.0 ± 8.0

[a] For meaning of A, B, C, k_{-1} and k_2, see Schemes III and IV and text; the pseudo-first-order rate constant k_1^{NMR} of the disappearance of A is directly obtained from the line shape simulation. The standard deviations of the stated temperatures were assumed to be ±1 K.

The simulation of the NMR line shapes in Figure 15 with the program DNMR3[67] according to the proposed kinetic Scheme IV yields the rate constant k_2 of reaction BC → CB in the concentration-independent degenerate equilibrium BC ⇌ CB. In addition, a pseudo-first-order rate constant k_1^{NMR} which corresponds to the disappearance of the monomer A is obtained. The rate constants k_1 and k_{-1} from Scheme IV and k_1^{NMR} are related as eq 6–11.

$$\frac{d[A]}{dt} = -2k_1[A]^2 + k_{-1}[BC] + k_{-1}[CB] \qquad (6)$$

Since [BC] = [CB], it follows

$$\frac{d[A]}{dt} = -2k_1[A]^2 + 2k_{-1}[BC] \qquad (7)$$

Under steady-state conditions eq 8 holds:

$$\frac{d[A]}{dt} = 0 \qquad (8)$$

and therefore

$$k_1[A]^2 = k_{-1}[BC] \qquad (9)$$

Since

$$k_1 = \frac{k_1^{NMR}}{[A]} \qquad (10)$$

it follows

$$k_{-1} = k_1^{NMR}\frac{[A]}{[BC]} \qquad (11)$$

(64) For calculation of thermodynamic data, the density of THF-d_8 was assumed to vary linearly between $d_4^{-109} = 1.023$ and $d_4^{20} = 0.887$ g/mL, cf. ref 54.

(65) MNDO values for H_2O and ethylenediamine (EDA): Kaufmann, E. University of Erlangen, FRG, unpublished results.

(66) MNDO calculations for a quantitative estimation of $\Delta S°$ of eq 4 are currently being carried out in our group. These take into account the possibility that dimer **24** is solvated by less than four THF ligands (Kaufmann, E.; Schleyer, P. v. R.; Bauer, W., unpublished results.)

(67) Kleier, D. A.; Binsch, G. DNMR3: Program no. 163, Quantum Chemistry Program Exchange (*QCPE*), Indiana University, 1969. We used a modified version of this program with real arithmetic.

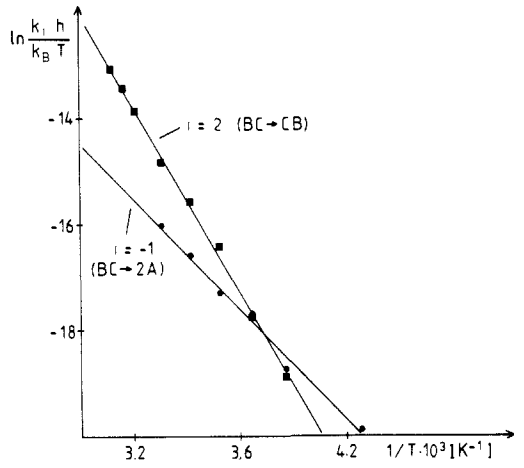

Figure 17. Eyring plot for the exchange reactions BC → CB and BC → 2A of the data from Table VII. For meaning of A, BC, CB, k_1, k_{-1}, and k_2, see Schemes III and IV and text; the calculation program ACTPAR[68] was used; h = Planck's constant; k_B = Boltzmann's constant; for standard deviations, see Table VII.

From eq 11 it follows that the rate constant k_{-1} can only be determined when the relative concentrations of A and BC are known. These can be obtained from the signal integrations in Figure 15 at low temperatures but must be extrapolated into the coalescence region. Therefore, to avoid systematic errors introduced by these extrapolations, we used only the low-temperature region for calculation of k_{-1} using eq 11 (see Table VII).

Figure 17 shows the Eyring plot ln $(k_i h/k_B T)$ versus $1/T$ of the data obtained experimentally for the monomer–dimer equilibrium (**3**·2TMEDA–**24**) and for the dimer interconversion of the dilithio product **3**. Least-squares analysis gives the activation parameters

$$\Delta H^{\ddagger}_{d,m} = 9.4 \pm 0.7 \text{ kcal/mol}$$

$$\Delta S^{\ddagger}_{d,m} = -23.5 \pm 2.5 \text{ eu}$$

for the reaction dimer **24** monomer → **3**·2TMEDA and

$$\Delta H^{\ddagger}_{d,d} = 16.1 \pm 0.4 \text{ kcal/mol}$$

$$\Delta S^{\ddagger}_{d,d} = 1.2 \pm 1.1 \text{ eu}$$

for the exchange of the lithium positions within the dimer **24**. For the former reaction, the large *negative* activation entropy can be rationalized by the participation of the chelating ligand, TMEDA, in the transition state leading from the dimer to the monomer. A mechanism involving a stepwise opening of the central C_4Li_4 moiety in dimer **24** with subsequent monohapto-like attachment of TMEDA to the vacant lithium coordination sites would be in agreement with the activation parameters. Thus, the intermediate leading from dimer **24** to monomer **3**·2TMEDA may be a mixed THF-d_8- and TMEDA-solvated species. Of particular interest are the activation parameters found for the exchange of the lithium positions in the dimer **24**. The near zero activation entropy of 1.2 ± 1.1 eu indicates a process *without* any association or dissociation of ligand molecules (THF-d_8 or TMEDA). A 180° reorientation of the "upper half" in the dimer **24** (i.e., by rotation of one monomer subunit) would lead to conversion of the lithium positions 1,1′ to 8,8′ and vice versa. This process might occur via initial dissociation into separate monomers, reorientation inside the solvent cage, and recombination.

At +25 °C, the Gibbs activation enthalpy for the lithium exchange process is $\Delta G_{298}^{\ddagger}$ = 15.7 kcal/mol. We can now understand the earlier findings concerning the barrier to exchange of the ortho and meta positions, respectively, in the nonlithiated aromatic ring of the dimer **24**: the experimental value due to pairwise coalescence of the ortho and meta protons of $\Delta G_{298}^{\ddagger}$ (exchange) = 15.2 kcal/mol agrees well with the value for the exchange of the lithium positions ($\Delta G_{298}^{\ddagger}$ (exchange) = 15.7 kcal/mol) but is much lower than the MNDO barrier to rotation

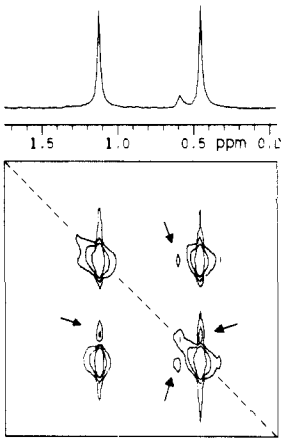

Figure 18. ^{6}Li–^{6}Li chemical exchange spectroscopy (NOESY pulse sequence), dissolved crystals of **3**·2TMEDA, THD-d_8, 0.2 M, −20 °C, mixing time 2.4 s, contour plot of nonsymmetrized absolute value spectrum.

of the nonlithiated aromatic ring in the *intact* dimer **25**. This means that the observed exchange of the ortho and meta protons H14,18 and H15,17, respectively, does *not* take place via rotation of the phenyl rings in the *intact* dimer. Instead, "180° reorientation of one monomer subunit" in **24** interchanges the "outer" and the "inner" ortho and meta positions of the nonlithiated aromatic rings in **24**. In this process, the observed coalescence in the ^{1}H and ^{13}C NMR spectrum is *not* related to rotation around the C1–C13 or the C1′–C13′ bonds.

The chemical exchange between different lithium sites within the dimer **24** and between dimer **24** and monomer **3**·2TMEDA (Scheme III) also is demonstrated with ^{6}Li–^{6}Li–2D NOESY spectra. The three-pulse NOESY sequence allows both the detection of nuclear Overhauser effects (NOE) and of chemical exchange of nuclei by two-dimensional spectroscopy.[19,69] We applied ^{6}Li–^{6}Li NOESY to the examination of the monomer **3**·2TMEDA dimer **24** equilibrium mixture in THF-d_8. Figure 18 shows the contour plot of the 2D–^{6}Li–^{6}Li exchange spectrum. At the recording temperature of −20 °C, the exchange rates k_2 and k_1 (Scheme III) are ca. 0.3 and 1.2 s^{-1}, respectively (cf. Table VII). For a mixing time of 2.4 s (in the order of the reciprocal of the rate constants[70]), intense exchange peaks are observed for the two ^{6}Li signals of the dimer **24**. Additional smaller exchange peaks (indicated with arrows in Figure 18) are observed for the ^{6}Li signals of the monomer **3**·2TMEDA. This confirms the assumptions in Scheme III: all lithium sites undergo mutual exchange.

Conclusions

Our study confirms and extends the results obtained by Mulvaney who used chemical methods for the structure analysis of the addition product of *n*BuLi and tolane. We have shown that a combination of spectroscopic methods (1D and 2D NMR, X-ray analysis) are an effective means for structure elucidation of subtle features of organolithium compounds. Thus, the qualitative and the quantitative behavior both as monomeric and as dimer dilithio compound **3** gave insight into the mechanisms of intra- and interaggregate exchange reactions. MNDO calculations, becoming ever more familiar to "lab chemists", are of great value for the evaluation and interpretation of experimental results and for the prediction of structures and to provide quantitative data (e.g., energies) which are not readily available experimentally.

Experimental Section

Instrumental. NMR spectra were recorded on a JEOL JNM GX 400 spectrometer under conditions previously described.[22] Measuring frequencies were 400 MHz (^{1}H), 100.6 MHz (^{13}C), and 58.8 MHz (^{6}Li).

(68) Binsch, G.; Kessler, H. *Angew. Chem., Int. Ed. Engl.* **1980**, *19*, 411.
(69) Meier, B. H.; Ernst, R. R. *J. Am. Chem. Soc.* **1979**, *101*, 6441.
(70) Derome, A. E. *Modern NMR Techniques for Chemistry Research*; Pergamon: Oxford, 1987; p 240.

Table VIII. Experimental Conditions of 2D NMR Spectra

figure	expt	temp [°C]	frequency range f_1 [Hz], f_2 [Hz]	scans per incrmnt	recrded incrmnt in t_1	filtering funcn[a] (t_1, t_2)	data matrix size (t_1, t_2)	delays[b] Δ_1, Δ_2 [ms]
1	^{1}H–^{1}H COSY, NOESY	−5	3171, 3171	64	128	SBELL, SBELL	256, 2048	mixing time 0.7 s (NOESY)
2a	C–H shift correlation	−5	3171, 20492	64	64	GAUS, GAUS	128, 4096	3.58, 1.79
2b	C–H shift correlation	−5	3171, 20492	64	160	GAUS, EXP	128, 4096	50.0, 30.0
4	^{6}Li–^{1}H HOESY	−30	3448, 200	16	64	GAUS, EXP	128, 512	mixing time 2.5 s
7	^{1}H–^{1}H COSY NOESY	−71	3161, 3161	32	96	SBELL, SBELL	256, 1024	mixing time 0.7 s (NOESY)
9a	C–H shift correlation	−71	3161, 15974	64	64	GAUS, GAUS	128, 4096	3.58, 1.79
9b	COLOC	−71	3161, 15974	128	128	GAUS, EXP	256, 2048	25.0, 30.0
11	^{6}Li–^{1}H HOESY	−71	3161, 100	16	96	GAUS, EXP	256, 512	mixing time 1.8 s
13	^{6}Li–^{6}Li COSY	−20	200, 200	32	40	GAUS, SSQUA	128, 512	400, 400
17	^{6}Li–^{6}Li NOESY	−20	200, 200	32	40	GAUS, SSQUA	128, 512	mixing time 2.4 s

[a] EXP = exponential line broadening; GAUS = Lorentzian to Gaussian transformation; SBELL = sine bell; SSQUA = squared sine bell. [b] Delays in the pulse sequence as described in ref 18 or in the original communications, respectively (see text).

A 5-mm ^{1}H/^{13}C probe and a 10-mm broad band probe were used. All samples were prepared in 5-mm tubes. One-dimensional ^{1}H and ^{13}C spectra were recorded typically by using 32 K data points and 5000 Hz or 25 000 Hz frequency range, respectively. Zero filling to 64 K data points was carried out where needed. Exponential line broadening of 0.1 and 1.5 Hz for ^{1}H and ^{13}C, respectively, was usually applied. One-dimensional ^{6}Li spectra were recorded without proton decoupling with a 45° pulse with 512 data points and 100 Hz frequency range. Zero filling to 1 K data points, where needed, was carried out. Exponential line broadening of 0.1 Hz was usually applied. The pulse delay for ^{6}Li was typically 6–8 s. Chemical shifts are reported in δ values (ppm) downfield from TMS and are referenced as follows: ^{1}H, [D$_7$H]–THF = 3.58 ppm, C$_6$D$_5$H = 7.15 ppm; ^{13}C, [D$_8$]THF = 67.4 ppm; C$_6$D$_6$ = 128.0 ppm as internal standards. ^{6}Li shifts are relative to 1 M LiBr in THF. The reference measurements were carried out separately before the sample measurements at the appropriate temperatures.

2D NMR Measurements. The pulse sequences for ^{1}H–^{1}H COSY,[18] ^{1}H–^{13}C chemical shift correlation,[18] ^{1}H–^{1}H NOESY,[20] ^{1}H–^{6}Li HOESY,[22] ^{6}Li–^{6}Li COSY,[58] and ^{6}Li–^{6}Li NOESY[20] measurements are described in the literature. Selected parameters of the recording conditions are summarized in Table VIII. Additional information is given in the figure captions. All 2D spectra are plotted in the absolute value mode. ^{1}H–^{1}H COSY/NOESY spectra were symmetrized after Fourier transformation.

X-ray Structure Analysis of 3·2TMEDA. Syntex P2$_1$ diffractometer, graphite monochromatized Mo Kα radiation, λ = 0.71069 Å, T = −35 °C. Crystal structure data: $C_{30}H_{50}Li_2N_4$, M_r = 480.64, monoclinic, space group $P2_1/n$ (no. 14), a = 14.507 (2) Å, b = 13.239 (2) Å, c = 16.756 (3) Å, β = 104.56 (1)°, V = 3114.8 Å^3, Z = 4, d_{calcd} = 1.025 g/cm^3, μ(Mo Kα) 0.6 cm^{-1}, F(000) = 1056. The intensities of 4751 reflections were recorded up to $(\sin\theta/\lambda)_{max}$ = 0.550 ($+h,+k,\pm l$, ω scan, $\Delta\omega$ = 0.8°). After Lp corrections and merging of equivalent data 4334 unique structure factors remained, 2984 of which with $F_o > 4.0\sigma(F_o)$ were deemed "observed" and used for all further calculations. The structure was solved by direct methods (SHELXS-86). The positions of 40 hydrogen atoms could be taken from difference maps, six were calculated at idealized geometrical positions. The H atoms at the disordered $(CH_2)_2$ moiety of one TMEDA ligand were neglected. Refinement with anisotropic displacement factors for the non-H atoms converged at $R(R_w)$ = 0.084 (0.081), $w = 1/\sigma^2(F_o)$ (H atoms constant with U_{iso} = 0.05 Å^2, one disordered CH_2 group isotropically in two alternatives; SHELX-76). The final difference map showed maxima of 0.68 e/Å^3, at the disordered TMEDA ligand, but was featureless otherwise. Table IV contains important distances and angles; Figure 6 shows the molecular structure. Further crystal structure data are available as Supplementary Material (see Supplementary Material paragraph at the end of paper).

MNDO Calculations were carried out with the AMPAC[71] program and lithium parametrization[72] on CYBER 855 and CONVEX C1 computers.

(71) The Dewar Research Group and J. J. P. Stewart: Quantum Chemistry Program Exchange, no. 506, 1986.
(72) Thiel, W.; Clark, T., unpublished (see the MNDOC program: Thiel, W.; Quantum Chemistry Program Exchange, no. 438).

1-Lithio-1,2-diphenylhex-1-ene (2), in Situ Preparation. Diphenylacetylene (87 mg, 0.49 mmol) was placed in a dry 5-mm NMR tube. This was fitted with a serum cap and evacuated. Drying was achieved by gently heating underneath the melting point of tolane (60 °C). After cooling and purging with argon, 0.3 mL of THF-d_8 (dried over sodium/lead alloy) was added via a syringe. In a separate flame-dried 5-mL flask under argon, 0.4 mL (0.5 mmol) of a 1.22 M n-butyllithium/hexane solution (enriched 96% with ^{6}Li; for preparation, see ref 26) was placed, and the solvent was evaporated in vacuo at room temperature. The residual oil was dissolved at ca. −60 °C in 0.4 mL of THF-d_8 and quickly syringed into the precooled (0 °C) THF-d_8–tolane solution. The reaction mixture was shaken carefully. A green color appeared. After ca. 4 h at −5 °C the reaction was completed (^{1}H NMR monitoring).

1,8-Dilithio-1,2-diphenylhex-1-ene·2TMEDA,3·2TMEDA. In a flame dried 25-mL flask under argon, 2.15 g (12.1 mmol) of diphenylacetylene, 8 mL of hexane, and 4.5 mL (30.0 mmol) of TMEDA (distilled from CaH_2, stored over CaH_2) were introduced. When the resulting clear solution was cooled to 0 °C, tolane precipitated. To the heterogeneous mixture at 0 °C, 15 mL (22.5 mmol) of an n-butyllithium/hexane solution 1.5 M) was added during ca. 10 min. The clear red solution was kept without stirring at room temperature. After 8 h, brown-red crystals formed. The mother liquor was removed by means of a syringe, and the crystals were washed with 15 mL of hexane in several portions. Drying in vacuo at room temperature yielded crystals suitable for X-ray analysis. Crystals for NMR analysis were prepared similarly, by using ^{6}Li-enriched n-butyllithium.[26]

Acknowledgment. We thank the Deutsche Forschungsgemeinschaft, the Convex Corporation, and the Fonds der Chemischen Industrie for financial support, Dr. T. Clark and E. Kaufmann for discussions, Prof. G. Fraenkel for critical comments, and the referees for suggestions.

Note Added in Proof. Recently, Günther et al. reported observations analogous to those shown in Figure 8 in this paper, i.e., the occurrence of ^{13}C NMR signals which show complex splittings due to coupling with chemically nonequivalent ^{6}Li nuclei (Gais, H.-J.; Vollhardt, J.; Günther, H.; Moskau, D.; Lindner, H. J.; Braun, S. *J. Am. Chem. Soc.* **1988**, *110*, 978). A review article dealing with modern NMR spectroscopy of organolithium compounds has recently been published by the same group: Günther, H.; Moskau, D.; Bast, P.; Schmalz, D. *Angew. Chem., Int. Ed. Engl.* **1987**, *26*, 1212.

Registry No. 1, 501-65-5; **2**, 115462-34-5; **3**, 35779-22-7; n-BuLi, 109-72-8; ^{6}Li, 14258-72-1.

Supplementary Material Available: Complete tables of atomic coordinates and displacement factors for (*E*)-1,8-dilithio-1,2-diphenylhex-1-ene (3·2TMEDA) (6 pages); lists of observed and calculated structure factor amplitudes (17 pages). Ordering information is given on any current masthead page.